

Forecasting range shifts of a dioecious plant species under climate change

Jacob K. Moutouama 0000-0003-1599-1671^{*1}, Aldo Compagnoni 0000-0001-8302-7492², and Tom E.X. Miller 0000-0003-3208-6067¹

¹Program in Ecology and Evolutionary Biology, Department of BioSciences, Rice University, Houston, TX USA

²Institute

of Biology, Martin Luther University Halle-Wittenberg, Halle, Germany; and German Centre for Integrative Biodiversity Research (iDiv), Leipzig, Germany

Running header: Forecasting range shifts

Keywords: demography, forecasting, global warming, matrix projection model, population dynamics, sex ratio, range limits

Submitted to: *Ecology letters* (Letter)

Data accessibility statement: All data used in this paper are publicly available and cited appropriately (Miller and Compagnoni, 2022a). Should the paper be accepted, all computer scripts supporting the results will be archived in a Zenodo package, with the DOI included at the end of the article. During peer review, our code (Stan, Bash and R) is available at <https://github.com/jmoutouama/POAR-Forecasting>.

Conflict of interest statement: None.

Authorship statement: J.K.M., A.C. and T.E.X.M. designed the study. A.C. and T.E.X.M. collected the data. All authors conducted the statistical analyses and modeling. J.K.M. drafted the manuscript, and T.E.X.M contributed to revisions.

Abstract:

Main Text:

Figures: 6

Tables: 0

References: 106

*Corresponding author: jmoutouama@gmail.com

¹ Abstract

² Global climate change has triggered an urgent need for predicting the reorganization of Earth's
³ biodiversity. Currently, the vast majority of models used to forecast population viability and
⁴ range shifts in response to climate change ignore the complication of sex structure, and thus
⁵ the potential for females and males to differ in their sensitivity to climate drivers. We developed
⁶ demographic models of range limitation, parameterized from geographically distributed com-
⁷ mon garden experiments, with females and males of a dioecious grass species (*Poa arachnifera*)
⁸ throughout and beyond its range in the south-central U.S. Female-dominant and two-sex
⁹ model versions both predict that future climate change will alter population viability and
¹⁰ will induce a poleward niche shift beyond current northern limits. However, the magnitude of
¹¹ niche shift was underestimated by the female-dominant model, because females have broader
¹² temperature tolerance than males and become mate-limited under female-biased sex ratios.
¹³ Our result illustrate how explicit accounting for both sexes could enhance population viability
¹⁴ forecasts and conservation planning for dioecious species in response to climate change.

¹⁵ Introduction

¹⁶ Rising temperatures and extreme drought events associated with global climate change are
¹⁷ leading to increased concern about how species will become redistributed across the globe
¹⁸ under future climate conditions (Bertrand et al., 2011; Gamelon et al., 2017; Smith et al., 2024).
¹⁹ Species' range limits, when not driven by dispersal limitation, should generally reflect the limits
²⁰ of the ecological niche (Lee-Yaw et al., 2016). Niches and geographic ranges are often limited
²¹ by climatic factors including temperature and precipitation (Sexton et al., 2009). Therefore,
²² any substantial changes in the magnitude of these climatic factors could impact population
²³ viability, with implications for range expansions or contractions based on which regions of
²⁴ a species' range become more or less suitable (Davis and Shaw, 2001; Pease et al., 1989).

²⁵ Forecasting range shifts for dioecious species (most animals and ca. 7% of plant species)
²⁶ is complicated by the potential for sexual niche differentiation, i.e. distinct responses of
²⁷ females and males to shared climate drivers (Hultine et al., 2016; Morrison et al., 2016; Pottier
²⁸ et al., 2021; Tognetti, 2012). ¹ Accounting for sexual niche differentiation is a long-standing
²⁹ challenge in accurately predicting which sex will successfully track environmental change
³⁰ and how this will impact population viability and range shifts (Gissi et al., 2023; Jones et al.,
³¹ 1999). Populations in which males are rare under current climatic conditions could experience
³² low reproductive success due to sperm or pollen limitation that may lead to population
³³ decline in response to climate change that disproportionately favors females (Eberhart-Phillips
³⁴ et al., 2017). In contrast, climate change could expand male habitat suitability (e.g. upslope
³⁵ movement), which might increase seed set for mate-limited females and favor range expansion
³⁶ (Petry et al., 2016). Across dioecious plants, for example, studies suggest that future climate
³⁷ change toward hotter and drier conditions may favor male-biased sex ratios (Field et al.,
³⁸ 2013; Hultine et al., 2016). ² Although the response of species to climate warming is an urgent
³⁹ and active area of research, few studies have disentangled the interaction between sex and
⁴⁰ climate drivers to understand their combined effects on population dynamics and range shifts,
⁴¹ despite calls for such an approach (Gissi et al., 2023; Hultine et al., 2016).

⁴² The vast majority of theory and models in population biology, including those used
⁴³ to forecast biodiversity responses to climate change, ignore the complication of sex structure
⁴⁴ (but see Ellis et al., 2017; Gissi et al., 2024; Pottier et al., 2021). Traditional approaches instead
⁴⁵ focus exclusively on females, assuming that males are in sufficient supply as to never limit
⁴⁶ female fertility. In contrast, "two-sex" models are required to fully account for demographic

¹ Something this paragraph is missing is a mechanistic explanation for why females and males may have different climate sensitivity, likely something about costs of reproduction. This would be a good place for a sentence or two that addresses this.

² I am not sure if this is the best spot for it, but I think this prediction from the literature is relevant to bring up in the Intro.

47 differences between females and males and sex-specific responses to shared climate drivers
48 (Gerber and White, 2014; Miller et al., 2011). Sex differences in maturation, reproduction,
49 and mortality schedules can generate skew in the operational sex ratio (OSR; sex ratio of
50 individuals available for mating) even if the birth sex ratio is 1:1 (Eberhart-Phillips et al., 2017;
51 Shelton, 2010). Climate and other environmental drivers can therefore influence the OSR
52 via their influence on sex-specific demographic rates. In a two-sex framework, demographic
53 rates both influence and respond to the OSR in a feedback loop that makes two-sex models
54 inherently nonlinear and more data-hungry than corresponding female-dominant models.
55 Given the additional complexity and data needs, forecasts of range dynamics for dioecious
56 species under future climate change that explicitly account for females, males, and their
57 inter-dependence are limited (Lynch et al., 2014; Petry et al., 2016).

58 Tracking the impact of climate change on population viability (λ) and distributional
59 limits of dioecious taxa depends on our ability to build mechanistic models that take into
60 account the spatial and temporal context of sex specific response to climate change, while
61 accounting for sources of uncertainty (Davis and Shaw, 2001; Evans et al., 2016). Structured
62 population models built from demographic data collected from geographically distributed
63 observations or common garden experiments provide several advantages for studying
64 the impact of climate change on species' range shifts (Merow et al., 2017; Schultz et al.,
65 2022; Schwinning et al., 2022). First, demographic models link individual-level life history
66 events (mortality, development, and regeneration) to population demography, allowing the
67 investigation of factors explaining vital rate responses to environmental drivers (Dahlgren
68 et al., 2016; Ehrlén and Morris, 2015; Louthan et al., 2022). Second, demographic models
69 have a natural interface with statistical estimation of individual-level vital rates that provide
70 quantitative measures of uncertainty and isolate different sources of variation, features that
71 can be propagated to population-level predictions (Elderd and Miller, 2016; Ellner et al.,
72 2022).³ Finally, structured demographic models can be used to identify which aspects of
73 climate are the most important drivers of population dynamics. For example, Life Table
74 Response Experiments (LTRE) built from structured models have become widely used to
75 understand the relative importance of covariates in explaining variation in population growth
76 rate (Czachura and Miller, 2020; Ellner et al., 2016; Hernández et al., 2023).⁴

77 In this study, we combine geographically-distributed common garden experiments,
78 hierarchical Bayesian statistical modeling, two-sex population projection modeling, and climate
79 back-casting and forecasting to understand demographic responses to climate change and

³I cut the sentence about experiments because I don't think our data really exemplify this. While we did do an experiment, we did not manipulate climate, so we are subject to the same correlations as observational studies.

⁴I think LTRE is a relatively small part of the paper so I suggested reducing the amount of text on it here.

their implications for past, present, and future range dynamics. Our work focused on the dioecious plant Texas bluegrass (*Poa arachnifera*), which is distributed along environmental gradients in the south-central U.S. corresponding to variation in temperature across latitude and precipitation across longitude (Fig. 1). This region has experienced rapid climate warming since 1900 and this is projected to continue through the end of the century (Fig. ??). Our previous study showed that, despite evidence for differentiation of climatic niche between sexes, the female niche mattered the most in driving longitudinal range limits of Texas bluegrass (Miller and Compagnoni, 2022b). However, that study used a single proxy variable (longitude) to represent environmental variation related to aridity and did not consider variation in temperature, which is the much stronger dimension of forecasted climate change in this region (Fig. ??,??⁵). Developing a rigorous forecast for the implications of future climate change requires that we transition from implicit to explicit treatment of multiple climate drivers, as we do here. Leveraging the power of Bayesian inference, we take a probabilistic view of past, present, and future range limits by quantifying the probability of population viability ($Pr(\lambda \geq 1)$) in relation to climate drivers of demography, an approach that fully accounts for uncertainty arising from multiple sources of estimation and process error. Specifically, we asked:

1. What are the sex-specific vital rate responses to variation in temperature and precipitation across the species' range?
2. How do sex-specific vital rates combine to determine the influence of climate variation on population growth rate (λ)?
3. What is the impact of climate change on operational sex ratio throughout the range?
4. What are the likely historical and projected dynamics of the Texas bluegrass geographic niche and how does accounting for sex structure modify these predictions?

Materials and methods

Study species and climate context

Texas bluegrass (*Poa arachnifera*) is a dioecious perennial, summer-dormant cool-season (C3) grass that occurs in the south-central U.S. (Texas, Oklahoma, and southern Kansas) (Figure 1) (Hitchcock, 1971). Texas bluegrass grows between October and May, flowers in spring, and goes dormant during the hot summer months of June to September (Kindiger, 2004). Following this life history, we divide the calendar year into growing (October 1 - May 31) and dormant (June 1 - September 30) seasons in the analyses below. Biological sex is genetically

⁵Please improve the legend for these figures.

111 based and the birth (seed) sex ratio is 1:1 (Renganayaki et al., 2005). Females and males are
112 morphologically indistinguishable except for their inflorescences. Like all grasses, this species
113 is wind pollinated (Hitchcock, 1971) and most male-female pollen transfer occurs within
114 10–15m (Compagnoni et al., 2017). Surveys of 22 natural populations throughout the species'
115 distribution indicated that operational sex ratio (the female fraction of inflorescences) ranged
116 from 0.007 to 0.986 with a mean of 0.404 (Miller and Compagnoni, 2022b).

117 Latitudinal limits of the Texas bluegrass distribution span 7.74 °C to 16.94 °C of
118 temperature during the dormant season and 24.38 °C to 28.80 °C during the dormant season.
119 Longitudinal limits span 244.9 mm to 901.5 mm of precipitation during the growing season
120 and 156.3 mm to 373.3 mm. This region has experienced *ca.* 0.5 °C of climate warming since
121 1900, with faster warming during the cool-season months (0.0055°C/yr) than the hot summers
122 (0.0046°C/yr) (Fig. S-1). Future warming is projected to accelerate to 0.03 – 0.06°C/yr by
123 the end of the century depending on the season and forecast model. On the other hand,
124 precipitation has increased over the past century for much of the region but is forecasted
125 to decline back to early-20th century levels (Fig. S-1).⁶

126 Common garden experiment

127 Experimental design

128 We conducted a range-wide common garden experiment to quantify sex-specific demographic
129 responses to climate variation. Details of the experimental design are provided in Miller
130 and Compagnoni (2022b); we provide a brief overview here. The experiment was installed
131 at 14 sites throughout and, in some cases, beyond the natural range of Texas bluegrass that
132 sampled a broad range of latitude and longitude (Figure 1A). At each site, we established
133 14 blocks. For each block we planted three female and three male individuals that were
134 clonally propagated from females and males from eight natural source populations (Figure
135 1A); because sex is genetically-based, clones never deviated from their expected sex. The
136 experiment was established in November 2013 with a total of # female and # male plants⁷,
137 and was censused in May of 2014, 2015, and 2016. At each census, we collected data on
138 survival, size (number of tillers), and number of panicles (reproductive inflorescences). For
139 the analyses that follow, we focus on the 2014–15 and 2015–16 transition years, since the start
140 of the experiment did not include the full 2013–14 transition year.

⁶Rather than just describe climate, this would be a good place to say more about climate change, which I have added. All of this sets the stage for why this is an important system to forecast climate change responses. If you think it is better we could move this to Results, since it is based on the climate data you describe below. I would like to figure out why the time series figure showed no change in precipitation but the past-present-future normals show a big change.

⁷Add numbers.

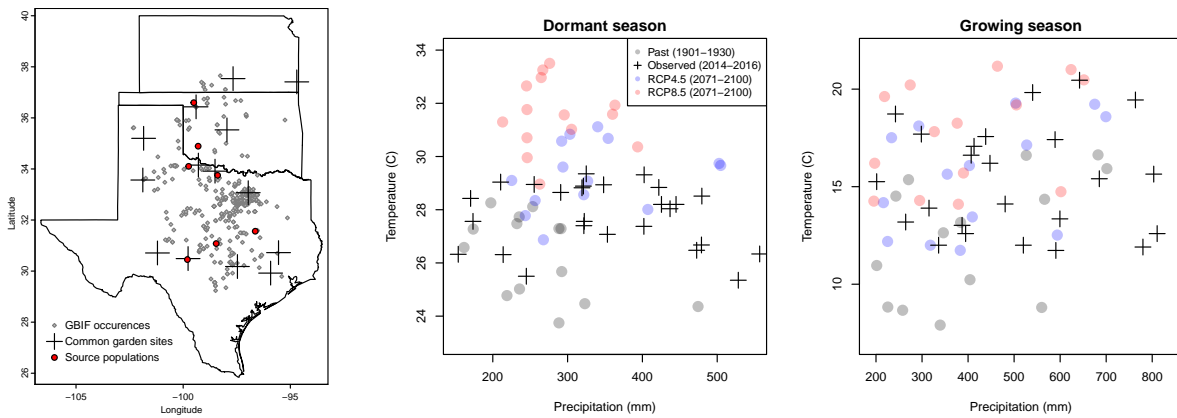


Figure 1: Experimental gardens and climate of the study region. **A:** Map of 14 experimental garden sites (crosses) in Texas, Oklahoma, and Kansas relative to GBIF occurrences of *Poa arachnifera* (gray points). Red points indicate source populations for plants used in the common garden experiment. **B,C:** Past, future, and observed climate space for growing and dormant seasons. Crosses show observed conditions for the sites and years of the common garden experiment. Gray points show historical (1901–1930) climate normals, and blue and red points show end-of-century (2071–2100) climate normals for RCP4.5 and RCP8.5 projections, respectively, from MIROC5. See also (Figure ?? for more information about historical and projected climate change in the study region.

141 Climatic data collection

142 We gathered downscaled monthly temperature and precipitation for each site from Chelsa
 143 (Karger et al., 2017) to describe observed climate conditions during our study period. These
 144 climate data were used as covariates in vital rate regressions. We aligned the climatic years
 145 to match demographic transition years (June 1 – May 31) and growing and dormant seasons
 146 within each year. To back-cast and forecast demographic responses to changes in climate
 147 throughout the study region, we also gathered projection data for three 30-year periods:
 148 “past” (1901–1930), “current” (1990–2019) and “future” (2070–2100). Data for future climatic
 149 periods were downloaded from four general circulation models (GCMs) selected from
 150 the Coupled Model Intercomparison Project Phase 5 (CMIP5): Model for Interdisciplinary
 151 Research on Climate (MIROC5), Australian Community Climate and Earth System Simulator
 152 (ACCESS1-3), Community Earth System Model (CESM1-BGC), Centro Euro-Mediterraneo sui
 153 Cambiamenti Climatici Climate Model (CMCC-CM). All the GCMs were downloaded from
 154 Chelsa (Sanderson et al., 2015). We evaluated future climate projections from two scenarios of
 155 representative concentration pathways (RCPs): RCP4.5, an intermediate-to-pessimistic scenario
 156 assuming a radiative forcing amounting to 4.5 W m^{-2} by 2100, and RCP8.5, a pessimistic
 157 emission scenario which projects a radiative forcing of 8.5 W m^{-2} by 2100 (Schwalm et al.,
 158 2020; Thomson et al., 2011).

159 Projection data for the three 30-year periods included warmer or colder conditions than ob-
 160 served in our experiment, so extending our inferences to these conditions required some extrap-
 161 olation. However, across all sites, both study years were 1-2°C warmer than their correspond-
 162 ing “current” (1990-2019) temperature normals (Fig. S-2). Additionally, the 2014–15 growing
 163 season was generally wetter and cooler across the study region than 2015–16 (Fig. S-2). Com-
 164 bined, the geographic and inter-annual replication of the common garden experiment provided
 165 good coverage of most past and future conditions throughout the study region (Fig. 1B,C).

166 **Sex-specific demographic responses to climatic variation across common garden sites**

We used individual-level measurements of survival, growth (change in number of tillers), flowering, and number of panicles (conditional on flowering) to develop Bayesian mixed effect models describing how each vital rate varies as a function of sex, size, and four climate covariates (precipitation and temperature of growing and dormant season). These vital rate models included main effects of size (the natural log of tiller number), sex, and seasonal climate covariates. Climate variables were fit with second-degree polynomial functions to accommodate the possibility of hump-shaped relationships (reduced demographic performance at both extremes). We also included two-way interactions between sex and each climate driver and between temperature and precipitation within each season, and a three-way interaction between sex, temperature, and precipitation within each season. Vital rate models were fit with the same linear predictors for the expected value (μ) (Eq.1):

$$\begin{aligned}
 \mu = & \beta_0 + \beta_1 \text{size} + \beta_2 \text{sex} + \beta_3 \text{pptgrow} + \beta_4 \text{pptdorm} + \beta_5 \text{tempgrow} + \beta_6 \text{tempdorm} \\
 & + \beta_7 \text{pptgrow*sex} + \beta_8 \text{pptdorm*sex} + \beta_9 \text{tempgrow*sex} + \beta_{10} \text{tempdorm*sex} \\
 & + \beta_{11} \text{size*sex} + \beta_{12} \text{pptgrow*tempgrow} + \beta_{13} \text{pptdorm*tempdorm} \\
 & + \beta_{14} \text{pptgrow*tempgrow*sex} + \beta_{15} \text{pptdorm*tempdorm*sex} + \beta_{16} \text{pptgrow}^2 \\
 & + \beta_{17} \text{pptdorm}^2 + \beta_{18} \text{tempgrow}^2 + \beta_{19} \text{tempdorm}^2 + \beta_{20} \text{pptgrow}^2 * \text{sex} \\
 & + \beta_{21} \text{pptdorm}^2 * \text{sex} + \beta_{22} \text{tempgrow}^2 * \text{sex} + \beta_{23} \text{tempdorm}^2 * \text{sex} + \phi + \rho + \nu
 \end{aligned} \tag{1}$$

167 The linear predictor includes normally distributed random effects for block-to-block variation
 168 ($\phi \sim N(0, \sigma_{block})$), site to site variation ($\nu \sim N(0, \sigma_{site})$), and source-to-source variation that
 169 is related to the genetic provenance of the transplants used to establish the common garden
 170 ($\rho \sim N(0, \sigma_{source})$).

171 A different link function ($f(\mu)$) was applied depending on the the vital rate distributions.
 172 We modeled survival and flowering data with a Bernoulli distribution. We modeled the
 173 growth (tiller number) with a zero-truncated Poisson inverse Gaussian distribution. Fertility

¹⁷⁴ (panicle count conditional on flowering) was modeled as zero-truncated negative binomial.
¹⁷⁵ We used generic, weakly informative priors to fit coefficients for survival, growth, flowering
¹⁷⁶ models ($\beta \sim N(0,1.5)$) and random effect variances ($\sigma \sim Gamma(\gamma(0.1,0.1))$). **We fit fertility**
¹⁷⁷ **model with regularizing priors for coefficients ($\mu=0, \sigma=0.15$)**.⁸

¹⁷⁸ **Sex ratio responses to climatic variation across common garden sites**

⁹ We also used the experimental data to investigate how climatic variation across the range influenced sex ratio and operational sex ratio of the common garden populations. To understand the impact of climate change on sex ratio, we used two methods. First, we developed eight Bayesian linear models using data collected during three years. Each model had OSR or SR as response variable and a climate variable as predictor (Eq.2).

$$SR = \omega_0 + \omega_1 climate + \omega_2 climate * climate + \epsilon \quad (2)$$

¹⁷⁹ where SR is the proportion of panicles that were female or proportion of female individuals
¹⁸⁰ in the experimental populations. ω_0 is the intercept, ω_1 and ω_2 are the climate dependent
¹⁸¹ slopes. ϵ is error term.

¹⁸² **Model-fitting procedures**

¹⁸³ All models were fit using Stan (Stan Development Team, 2023) in R 4.3.1 (R Core Team,
¹⁸⁴ 2023). We centered and standardized all climatic predictors to mean zero, variance one, which
¹⁸⁵ facilitated model convergence. We ran three chains for 1000 samples for warmup and 4000
¹⁸⁶ for sampling, with a thinning rate of 3. We assessed the quality of the models using posterior
¹⁸⁷ predictive checks (Piironen and Vehtari, 2017) (Figure S-3).

¹⁸⁸ **Two-sex and female-dominant matrix projection models**

¹⁸⁹ We used the climate-dependent vital rate regressions estimated above, combined with
¹⁹⁰ additional data sources, to build female-dominant and two-sex versions of a climate-explicit
¹⁹¹ matrix projection model (MPMs) structured by the discrete state variables size (number
¹⁹² of tillers) and sex. The female-dominant and two-sex versions of the model both allow
¹⁹³ for sex-specific response to climate and differ only in the feedback between operational
¹⁹⁴ sex ratio and seed fertilization. For clarity of presentation we do not explicitly include

⁸ I think you need to explain a little more about why fertility was handled differently and what you mean by regularizing.

⁹ This section will need to be updated with the new model.

¹⁹⁵ climate-dependence in the notation below, but the following model was evaluated over
¹⁹⁶ variation in seasonal temperature and precipitation.

Let $F_{x,t}$ and $M_{x,t}$ be the number of female and male plants of size x in year t , where $x \in [1, \dots, U]$. The minimum possible size is one tiller and U is the 95th percentile of observed maximum size (# tillers)¹⁰. Let F_t^R and M_t^R be new female and male recruits in year t , which we treat as distinct from the rest of the size distribution because we assume they do not reproduce in their first year, consistent with our observations. For a pre-breeding census, the expected numbers of recruits in year $t+1$ is given by:

$$F_{t+1}^R = \sum_L^U [p^F(x) \cdot c^F(x) \cdot d \cdot v(\mathbf{F}_t, \mathbf{M}_t) \cdot m \cdot \rho] F_{x,t} \quad (3)$$

$$M_{t+1}^R = \sum_L^U [p^F(x) \cdot c^F(x) \cdot d \cdot v(\mathbf{F}_t, \mathbf{M}_t) \cdot m \cdot (1-\rho)] F_{x,t} \quad (4)$$

¹⁹⁷ where p^F and c^F are flowering probability and panicle production for females of size x , d
¹⁹⁸ is the number of seeds per female panicle, v is the probability that a seed is fertilized, m is
¹⁹⁹ the probability that a fertilized seed germinates, and ρ is the primary sex ratio (proportion
²⁰⁰ of recruits that are female), which we assume to be 0.5¹¹.

In the two-sex model, seed fertilization is a function of population structure, allowing for feedback between vital rates and operational sex ratio (OSR). In the context of the model, OSR is defined as the fraction of panicles that are female and is derived from the $U \times 1$ vectors \mathbf{F}_t and \mathbf{M}_t :

$$v(\mathbf{F}_t, \mathbf{M}_t) = v_0 * \left[1 - \left(\frac{\sum_1^U p^F(x, z) c^F(x, z) F_{x,t}}{\sum_1^U p^F(x, z) c^F(x, z) F_{x,t} + p^M(x, z) c^M(x, z) M_{x,t}} \right)^\alpha \right] \quad (5)$$

²⁰¹ The summations tally the total number of female and male panicles over the size distribution,
²⁰² giving the fraction of total panicles that are female. We focus on the female fraction of
²⁰³ panicles and not female fraction of reproductive individuals because panicle number can vary
²⁰⁴ widely depending on size; we assume that few males with many panicles vs. many males
²⁰⁵ with few panicles are interchangeable pollination environments. Eq. 5 has the properties
²⁰⁶ that seed fertilization is maximized at v_0 as OSR approaches 100% male, goes to zero as OSR
²⁰⁷ approaches 100% female, and parameter α controls how female seed viability declines as male
²⁰⁸ panicles become rare. We estimated these parameters using data from a sex ratio manipulation
²⁰⁹ experiment, conducted in the center of the range, in which seed fertilization was measured
²¹⁰ in plots of varying OSR; this experiment is described elsewhere (Compagnoni et al., 2017) and

¹⁰ Give this number.

¹¹ I believe we can cite this - check the Am Nat paper.

211 is summarized in **Supplementary Method S.2**¹². This experiment also provided estimates for
 212 seed number per panicle (d) and germination rate (m). Lacking data on climate-dependence,
 213 we assume that seed fertilization, seed number, and germination rate do not vary with climate.

The dynamics of the size-structured component of the population are given by:

$$F_{y,t+1} = [\sigma \cdot g^F(y, x=1)] F_t^R + \sum_L^U [s^F(x) \cdot g^F(y, x)] F_{x,t} \quad (6)$$

$$M_{y,t+1} = [\sigma \cdot g^M(y, x=1)] M_t^R + \sum_L^U [s^M(x) \cdot g^M(y, x)] M_{x,t} \quad (7)$$

214 The first terms indicate recruits that survived their first year and enter the size distribution
 215 of established plants. We estimated the seedling survival probability σ using demographic
 216 data from the congeneric species *Poa autumnalis* in east Texas (T.E.X. Miller and J.A. Rudgers,
 217 *unpublished data*), and we assume that σ is the same across sexes and climatic variables. We did
 218 this because we had little information on the early life cycle transitions of greenhouse-raised
 219 transplants. We used $g(y, x=1)$ (the future size distribution of one-tiller plants from the
 220 transplant experiment) to give the probability that a surviving recruit reaches size y . The
 221 second component of the equations indicates survival and size transition of established
 222 plants from the previous year, where s and g give the probabilities of surviving at size x and
 223 growing from sizes x to y , respectively, and superscripts indicate that these functions may
 224 be unique to females (F) and males (M).

225 The model described above yields a $2(U+1) \times 2(U+1)$ transition matrix. We estimated
 226 the population growth rate λ of the female dominant model as the leading eigenvalue of
 227 the transition matrix. Since the two-sex MPM is nonlinear (matrix elements affect and are
 228 affected by population structure) we estimated λ and stable sex ratio (female fraction of all
 229 individuals) and operational sex ratio (female fraction of panicles) by numerical simulation.
 230 Since all parameters were estimated using MCMC sampling, we were able to propagate the
 231 uncertainty in our estimates of the vital rate parameters to uncertainty in λ . Furthermore,
 232 by sampling over distributions associated with site, block, and source population variance
 233 terms, we are able to incorporate process error into the total uncertainty in λ , in addition
 234 to the uncertainty that arises from imperfect knowledge of the parameter values. For example,
 235 sampling over site and block variances accounts for regional and local spatial heterogeneity
 236 that is not explained by climate, and sampling over source population variance accounts for
 237 genetically-based demographic differences across the species' range.¹³

¹²I think the supplement should also include a data figure showing the fit of the model to the experimental data.

¹³I just want to confirm that this is actually what you did.

238 **Life Table Response Experiments**

239 We conducted two types of Life Table Response Experiments (LTRE) to isolate contributions
240 of climate variables and sex-specific vital rates to variation in λ . First, to identify which
241 aspect of climate is most important for population viability, we used an LTRE based on
242 a nonparametric model for the dependence of λ on parameters associated with seasonal
243 temperature and precipitation (Ellner et al., 2016). To do so, we used the RandomForest
244 package to fit a regression model with four climatic variables (temperature of growing season,
245 precipitation of growing season, temperature of the dormant season and precipitation of
246 the dormant season) as predictors and λ^{14} as response (Liaw et al., 2002). The regression
247 model allowed the estimation of the relative importance of each predictor. **The importance**
248 **is measured by asking: how wrongly is λ predicted if we replaced the focal predictor (e.g.,**
249 **temperature of growing season) by a random value of the other predictors.**¹⁵

Second, to understand how climate drivers influence λ via sex-specific demography, we decomposed the effect of each climate variable on population growth rate (λ) into contribution arising from the effect on each female and male vital rate using a “regression design” LTRE (Caswell, 1989, 2000). This LTRE decomposes the sensitivity of λ to climate according to:

$$\frac{\partial \lambda}{\partial \text{climate}} \approx \sum_i \frac{\partial \lambda}{\partial \theta_i^F} \frac{\partial \theta_i^F}{\partial \text{climate}} + \frac{\partial \lambda}{\partial \theta_i^M} \frac{\partial \theta_i^M}{\partial \text{climate}} \quad (8)$$

250 where, θ_i^F and θ_i^M represent sex-specific parameters (the regression coefficients of the vital
251 rate functions). Because LTRE contributions are additive, we summed across vital rates to
252 compare the total contributions of female and male parameters.¹⁶¹⁷

253 **Population viability across the climatic niche and geographic range**

254 To understand how climate shapes the niche and geographic range of Texas bluegrass, we
255 estimated the probability of self-sustaining populations ($\Pr(\lambda \geq 1)$) conditional to temperature
256 and precipitation of the dormant and growing seasons. $\Pr(\lambda > 1)$ was calculated for the
257 two-sex model and the female dominant MPMs using the proportion of the 300 posterior
258 samples that lead to a $\lambda \geq 1$ (Diez et al., 2014). Population viability in climate niche space
259 was then represented as a contour plot with values of $\Pr(\lambda > 1)$ at given temperature and
260 precipitation for the growing season, holding dormant season climate constant, and vice versa.

¹⁴Is this lambda from the female-dominant or two-sex model? Does it matter?

¹⁵I do not understand this.

¹⁶ θ_i^F and θ_i^M include the interaction and second order effect. I think we are good with this formula

¹⁷I do not agree. It is true that you can compute this, but only by “turning off” the interaction by holding the interacting variable constant. I still think this needs to be better addressed in both LTRE analyses.

261 Pr ($\lambda > 1$) was also mapped onto geographic layers of three US states (Texas, Oklahoma
262 and Kansas) to delineate past, current and future potential geographic distribution of the
263 species. To do so, we estimated Pr ($\lambda > 1$) conditional to all climate covariates for each
264 pixel (~25 km²) for each time period (past, present, future). Because of the amount of the
265 computation involved, we use 100 posterior samples to estimate Pr ($\lambda > 1$) across the study
266 area (Texas, Oklahoma and Kansas).

267 To compare the probability of self-sustaining populations between the female dominant
268 and the two-sex model, we used a zero-inflated beta model in brms (Bürkner, 2017). ¹⁸

269 **Results**

270 **Sex specific demographic response and sex ratio variation across climatic
271 conditions**

272 We found strong demographic responses to climate drivers across our Texas bluegrass
273 common garden sites and years, and evidence for demographic differences between the
274 sexes. Regression coefficients related to sex and/or sex:size interactions were significantly
275 non-zero (95% credible intervals excluding zero) for most vital rates (Fig. S-4), suggesting
276 sexual divergence in demography. Females generally had an advantage over males, especially
277 in survival and flowering (Fig. 2). Vital rate regressions also revealed significant interactions
278 between sex and climate drivers, especially in vegetative growth (Fig. S-4)B. ¹⁹

¹⁸*This just floats here without much context. Not sure we need it, but I am flagging for now and will come back to this after reading the results.*

¹⁹*I am skipping the rest of this section for now because I think we need a different visualization for the vital rates. I also think this section should include the common garden sex ratio results, since they are connected to the vital rate responses.*

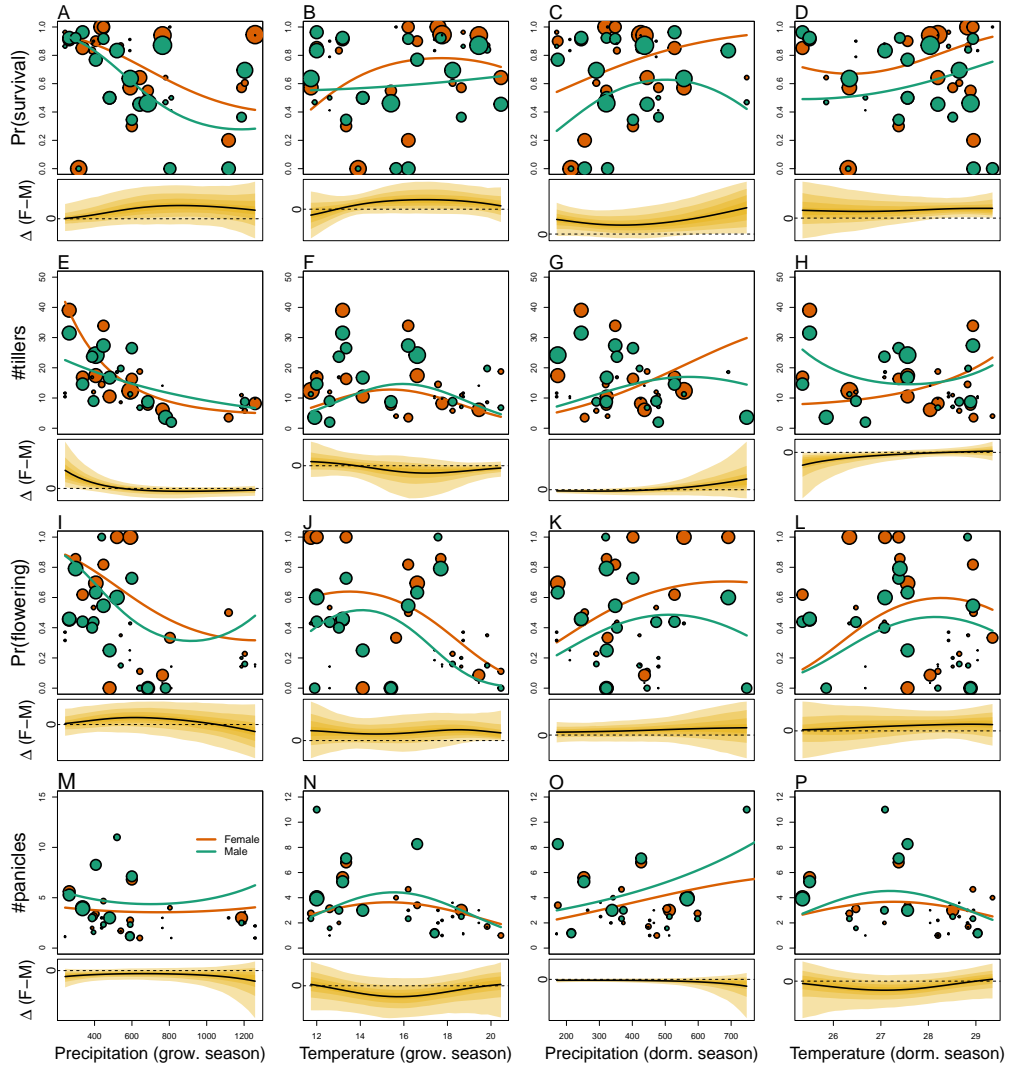


Figure 2: Sex specific demographic response to climate across species range. (A, B, C, D) Probability of survival as a function of precipitation and temperature of the growing and dormant season. (E, F, G, H) Change in number of tillers as a function of precipitation and temperature of the growing and dormant season. (I, J, K, L) Probability of flowering as a function of precipitation and temperature of growing and dormant season. (M, N, O, P) Change in number of panicles as a function of precipitation and temperature of the growing and dormant season. Points show means by site for females (orange) and males (green). Points sizes are proportional to the sample sizes of the mean and are jittered. Lines show fitted statistical models for females (orange) and males (green) based on posterior mean parameter values. Lower panels below each data panel show the posterior distribution of the difference between females and males as a function of climate (positive and negative values indicate female and male advantage, respectively); dashed horizontal line shows zero difference.

279 Across common garden sites, operational sex ratio (proportion of female panicles) of the
 280 experimental populations was female-biased on average (STATS), reflecting the overall greater
 281 rates of female vs. male flowering rather than bias in the underlying population composition

282 (all sites were planted with equal numbers of females and males). Across sites and years, OSR
283 variation was significantly predicted by [describe sex ratio analyses].²⁰

284 Climate drivers of population viability across niche space

285 Putting all vital rates together in the MPM framework reveals how climate shapes fitness
286 variation across niche dimensions and geographic space, and how accounting for sex structure
287 modifies these inferences. Figure 3 shows the estimated probability of population viability
288 ($\lambda \geq 1$) across seasonal climate niche space; these probabilities account for uncertainty in the
289 vital rate parameters as well as process error related to spatial heterogeneity and genotypic
290 variation. For both female-dominant and two-sex models, fitness variation across niche space
291 was dominated by temperature, with weaker effects of precipitation (compare vertical and
292 horizontal contours in Fig. 3). These visual trends are supported by LTRE decomposition
293 indicating that variation in fitness across climatic conditions is most strongly driven by
294 responses to growing and dormant season temperature, with weaker interactive effects of
295 precipitation that modulate the effects of temperature (Figure S-10). LTRE analysis also showed
296 that declines in population viability at high and low temperatures were driven most strongly
297 by reductions in vegetative growth and panicle production, with stronger contributions from
298 females than males (Figure S-11).²¹ Intermediate temperatures of both growing and dormant
299 seasons were associated with near-certain projections of population viability ($Pr(\lambda \geq 1) \approx 1$),
300 and high and low temperature extremes during both seasons were associated with low niche
301 suitability ($Pr(\lambda \geq 1) < 0.2$). Higher precipitation slightly expanded the range of suitable
302 temperatures during the dormant season (Fig. 3A), and the reverse was true in the growing
303 season (Fig. 3B). Points in Fig. 3 show that climate change forecasted for the common
304 garden locations would move many of them toward lower-suitability regions of niche space
305 associated with high growing and dormant season temperatures (see also Fig. S-5).²²

306 While the female-dominant and two-sex models were generally in agreement about
307 high confidence in intermediate temperature optima, they differed around the edges of niche
308 space (Fig. 3C,D²³,S-5). The female-dominant model over-predicted population viability,
309 especially with respect to growing season temperature. For example, the female-dominant
310 model predicted²⁴ that, for most levels of precipitation, warm average growing season (winter)

²⁰I am not sure what the new sex ratio results look like, so not sure if we are keeping this.

²¹You can see here that I am suggesting we moved the lambda vs climate figure to an appendix. If you disagree we can keep it, but I think the niche space results are the better figure to show.

²²I think we should redraw this without contours so that the points are more readable. I would also change the point types and sizes.

²³All multi-panel figures need letter labels.

²⁴I think I am switching tenses. We will need to clean this up.

311 temperatures of $\sim 20^{\circ}\text{C}$ had high suitability ($Pr(\lambda \geq 1) > 0.9$), while the two-sex model
312 indicated that these conditions were most likely unsuitable ($Pr(\lambda \geq 1) < 0.5$). Similarly, at
313 low winter temperatures that the two-sex model identifies with high certainty as unsuitable
314 ($Pr(\lambda \geq 1) < 0.1$), the female-dominant model is more optimistic ($Pr(\lambda \geq 1) > 0.4$). Across
315 growing season climate space, the female-dominant model over-estimates population viability
316 by ca. 10%, on average (Fig. 3D, Fig. S-13B). The difference between female-dominant and
317 two-sex models was qualitatively similar but weaker in magnitude for niche dimensions of
318 the dormant season (Fig. 3C, Fig. S-13A).

319 Female-dominant and two-sex models diverged most strongly in regions of niche
320 space that favored strongly female-biased operational sex ratios (Fig. WE NEED A FIGURE
321 FOR THIS). This suggests mate limitation as the biological mechanism underlying model
322 differences. The two-sex model accounts for feedbacks between OSR and female fertility, with
323 reduced seed viability at OSR exceeding $\sim 75\%$ female panicles (Fig. WE NEED A FIGURE
324 FOR THIS). Lacking this feedback, the female-dominant model over-predicts population
325 viability in regions of niche space where male flowering is not sufficient to maximize seed set.

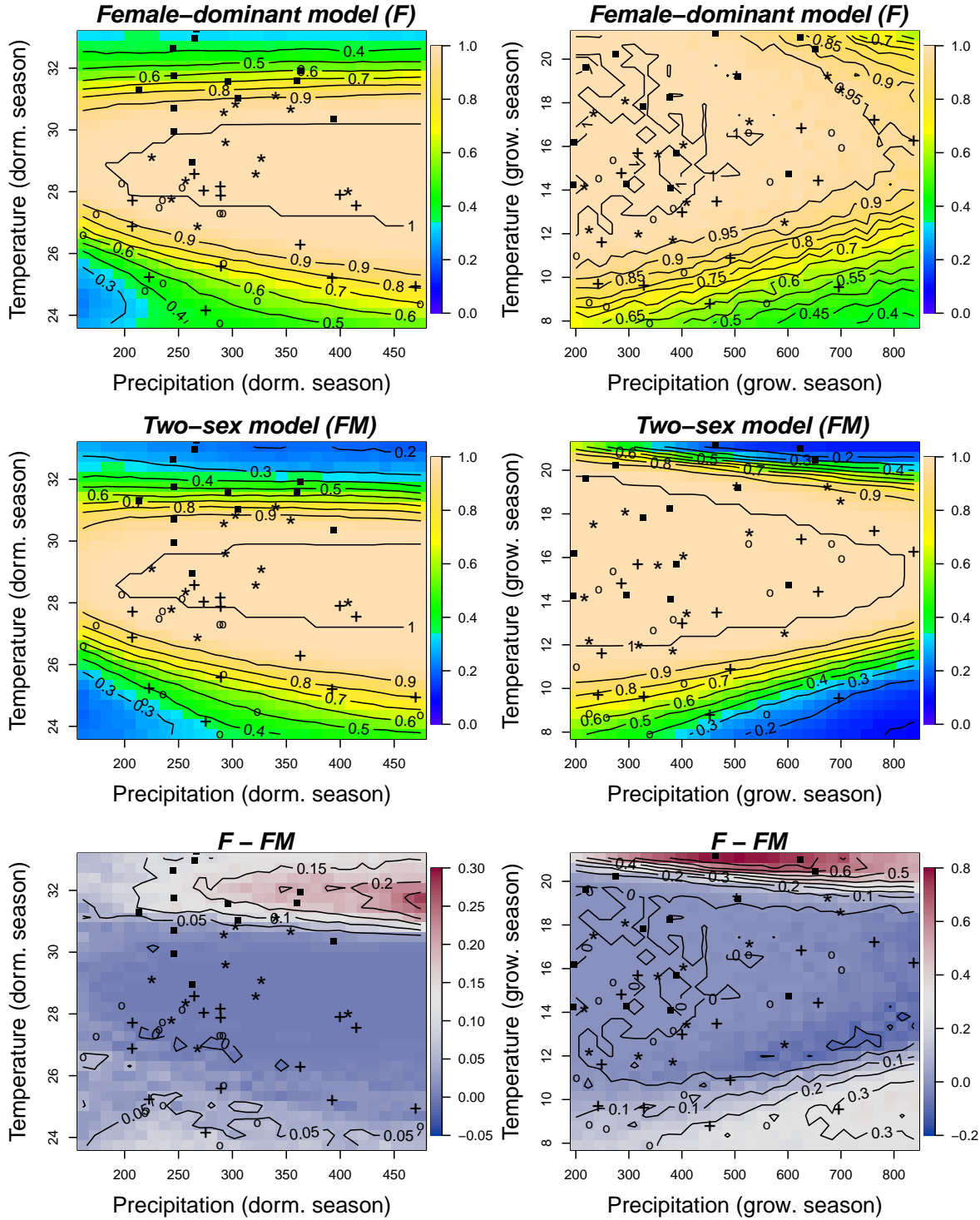


Figure 3: A two-dimensional representation of the predicted niche shift over time (past, present and future climate conditions). Contours on the first four panels show predicted probabilities of self-sustaining populations, $\Pr(\lambda > 1)$ conditional on precipitation and temperature of the dormant and growing season. The last two panels show difference in niche estimation between the female dominant model and the two-sex model for each season. "o": Past, "+" Current, "*": RCP 4.5, "■": RCP 8.5.

326 **Climatic change induces shifts in geographic niche and population OSR**

327 Projecting the climatic niche onto geographic space, we find that suitable niche conditions for
328 Texas bluegrass are shifting north under climate change (Fig. 4). Under past (1901-1930) and
329 present (1990-2019) conditions, the two-sex and female-dominant models predict widespread
330 suitability with high confidence ($Pr(\lambda \geq 1) \approx 1$) across much of Texas and Oklahoma. For
331 both models, the predicted geographic niche generally corresponds well to independent
332 observations of the Texas bluegrass distribution (Fig.²⁵). The predicted geographic niche is
333 more expansive than the observed distribution, particularly at southern, western, and eastern
334 edges, suggesting some degree of range disequilibrium (e.g., due to dispersal limitation),
335 geographic bias in occurrence observations, and/or model mis-specification. Comparing past
336 to present conditions, the geographic niche for both models has shifted slightly poleward,
337 with reductions in viability at the southern margins and expansions of viability at northern
338 margins. The northward shift of suitable niche conditions is even more pronounced in
339 projections to end-of-century (2071-2100) conditions, with the most dramatic changes in the
340 most pessimistic (RCP8.5) scenario (Fig.²⁶). In fact, under the pessimistic scenario, Texas
341 bluegrass will have very little remaining climate suitability in the state of Texas by the end
342 of the 21st century. The predicted poleward niche shift is consistent across different global
343 circulation models (Figure S-14, Figure S-15, Figure S-16).

344 Female-dominant and two-sex models are in broad agreement about northward
345 migration of the climatic niche, but the geographic projections reveal hotspots of disagreement
346 where the female-dominant model over-predicts climate suitability and under-predicts the
347 likelihood of range shifts (Fig. 4). These hotspots are generally regions of predicted female
348 bias in the operational sex ratio (Fig. WE NEED A FIGURE FOR THIS.) The strongest contrast
349 between the two models is in the pessimistic climate change scenario (RCP8.5), where the
350 female-dominant model over-predicts population viability by ca. 25%²⁷ across much of the
351 region (Fig. WE NEED A FIGURE SHOWING THE DISTRIBUTION OF THE DIFFERENCE)
352 and under-estimates the magnitude of a potential range shift. In this scenario, a broad swath
353 of the current distribution that is forecasted to be effectively unsuitable ($Pr(\lambda \geq 1) \approx 0$) by the
354 two-sex model is identified as marginally suitable ($Pr(\lambda \geq 1) \approx 0.5$) by the female-dominant
355 model. Accordingly, the OSR of Texas bluegrass across its range is projected to be ca. 75%
356 female panicles, on average, by end of century under RCP8.5, an increase from ca. 60% female
357 under projections for past and current conditions (Fig. 5). The more optimistic climate change
358 scenario (RCP4.5) predicts an intermediate shift in OSR, with hotspots of change becoming

²⁵ I think we should add the GBIF records to the map.

²⁶ Here and throughout, we need to reference specific figure panels by letter label.

²⁷ I just eyeballed this. Real number should come from the histograms.

³⁵⁹ strongly female-biased but most of the range remaining near current levels of 60% female
³⁶⁰ (Fig. 5; WE NEED A MAP SHOWING WHERE OSR IS BECOMING MORE BIASED).

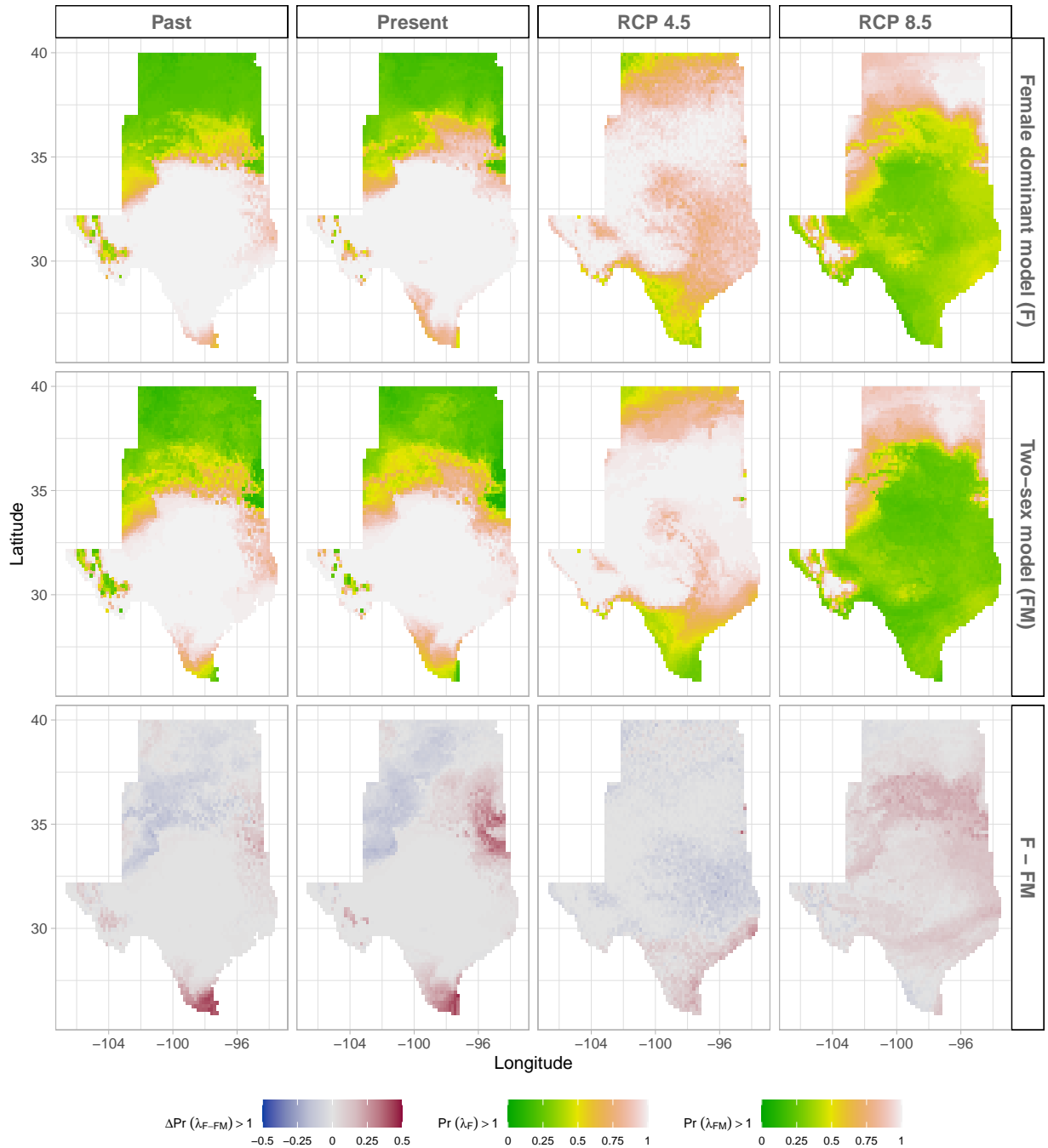


Figure 4: Climate change favors range shift towards north edge. (A) Past, (B) Current, (C and D) Future predicted range shift based on the predicted probabilities of self- sustaining populations, $\text{Pr}(\lambda > 1)$, using the two-sex model that incorporates sex- specific demographic responses to climate with sex ratio dependent seed fertilization. (E) Past, (F) Current, (G and H) Future predicted range shift based on the predicted probabilities of self- sustaining populations, $\text{Pr}(\lambda > 1)$, using the female dominant model. Future projections were based on the CMCC-CM model. The black dots on panel B and F indicate all known presence points collected from GBIF from 1990 to 2019, which corresponds to the current condition in our prediction. The occurrences of GBIFs are distributed in with higher population fitness habitat $\text{Pr}(\lambda \geq 1)$, confirming that our study approach can reasonably predict range shifts.

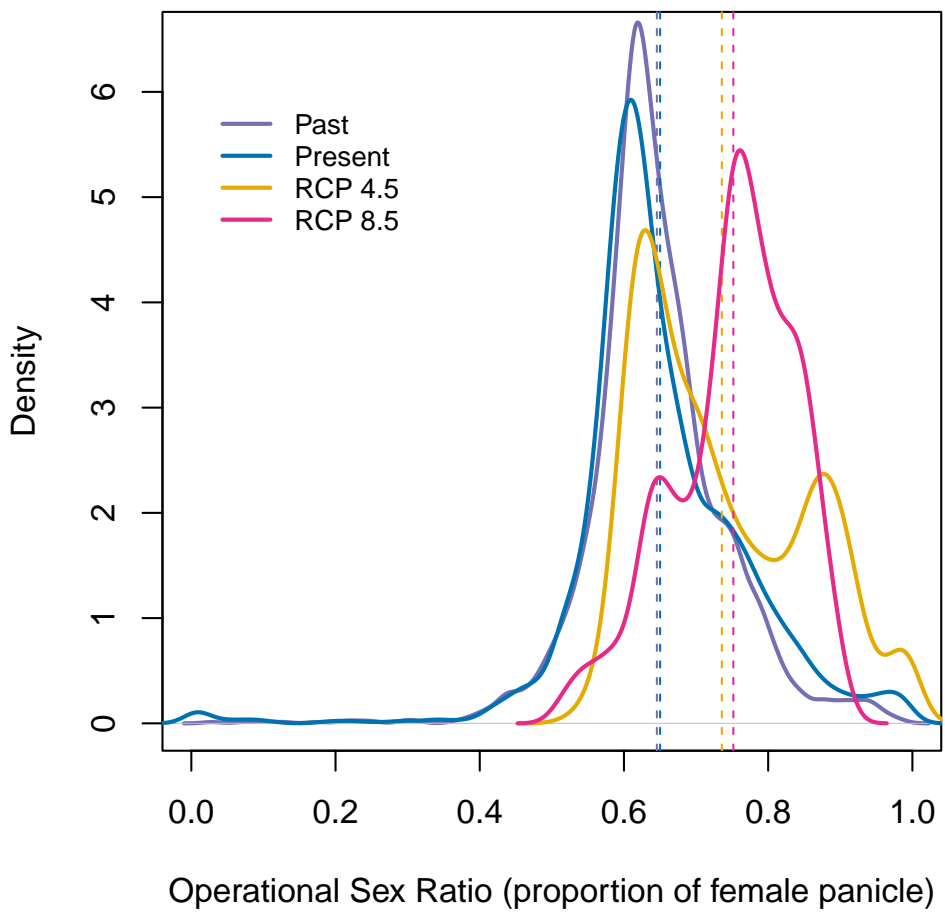


Figure 5: Change in Operational Sex Ratio (proportion of female panicle) over time (past, present, future). Future projections were based on the CMCC-CM model. The mean sex ratio for each time period is shown as vertical dashed line.

361 Discussion

362 Dioecious species make up a large fraction of Earth's biodiversity – most animals and many
 363 plants – yet we have little knowledge about how sex-specific demography and responses to
 364 climate drivers may affect population viability and range shifts of dioecious species under
 365 climate change.²⁸ We used demographic data collected common garden experiments and
 366 sex-structured demographic modeling to forecast for the first time the likely impact of climate
 367 change on range dynamics of a dioecious species. Our future projections require extrapolation
 368 to warmer or colder conditions than observed in our experiment and subsequently should be

²⁸*Love this opening sentence.*

369 interpreted with caution (Chen et al., 2024).²⁹ Three general patterns emerged from our analysis
370 of range-wide common garden experiments and sex-structured, climate-explicit demographic
371 models. First, our Bayesian mixed effect model suggests a sex specific demographic response
372 to climate change that lead to higher proportion of female as climate increase. Second, climate
373 change favors a northern range shifts in suitable habitats. Third, the female dominant model
374 (model that does not account for sex structure) overestimates species niche and range shifts.

375 There was a female demographic advantage leading to a female biased in response
376 to climate change in *Poa arachnifera* populations. The extreme female-bias in response to
377 climate change contrast with previous studies suggesting that an increase in male frequency
378 in response to climate change (Hultine et al., 2016; Petry et al., 2016). Two mechanisms
379 could explain the observed demographic advantage of females over males for survival and
380 flowering and the opposite for growth and number of panicles. The trade-off between fitness
381 traits (survival, growth and fertility) due to resource limitation and the pollination mode of
382 our study species (wind pollinated) could explain such a result (Cipollini and Whigham, 1994;
383 Freeman et al., 1976). For most species, the cost of reproduction is often higher for females
384 than males due to the requirement to develop seeds and fruits (Hultine et al., 2016). However,
385 several studies reported a higher cost of reproduction for males in wind pollinated species
386 due to the larger amounts of pollen they produce (Bruijning et al., 2017; Bürli et al., 2022;
387 Cipollini and Whigham, 1994; Field et al., 2013).

388 Our results suggest that climate change will alter population at the center of the range
389 and drive a northern range shifts. This impact of climate change on the species current
390 niche could be explained by the increase of temperature over the next years. Small change
391 in temperature of the growing and dormant season have a larger impact on population
392 viability. Temperature can impact plant populations through different mechanisms. Increasing
393 temperature could increase evaporative demand, affect plant phenology (Iler et al., 2019;
394 McLean et al., 2016; Sherry et al., 2007), and germination rate (Reed et al., 2021). The potential
395 for temperature to influence these different processes changes seasonally (Konapala et al.,
396 2020). For example, studies suggested that species that are active during the growing season
397 such as cool grass species can have delayed phenology in response to global warming,
398 particularly if temperatures rise above their physiological tolerances (Cleland et al., 2007;
399 Williams et al., 2015). In addition, high temperature during the growing season by affecting
400 pollen viability, fertilization could affect seed formation and germination (Hatfield and
401 Prueger, 2015; Sletvold and Ågren, 2015). Pollen dispersal may allow plants to resist climate
402 change because pollen dispersal may provide the local genetic diversity necessary to adapt
403 at the leading edge of the population (Corlett and Westcott, 2013; Duputié et al., 2012; Kremer

²⁹I think extrapolation should be its own paragraph. This also relates to uncertainty in the climate forecasts.

et al., 2012). Since wind pollination is most effective at short distances, it is most often found in plant species growing at high density such as our study species, it is less likely that dispersal limitation affect niche shift in our study system. Difference in non-climatic factors such as soil, or biotic interactions could also explain decline in population growth rate as an indirect effects of increase in temperature (Alexander et al., 2015; Schultz et al., 2022). For example, climate change could increase the strength of species competition and thereby constrain our study species to a narrower realized niche (Aguilée et al., 2016; Pulliam, 2000).

We found evidence of underestimation of the impact of climatic change on population dynamics by the female dominant model and implication for such an underestimation on conservation actions for dioecious species. The underestimation of the impact of climatic change on population dynamics by the female dominant model makes sense given the sex specific response to climatic change. *Poa arachnifera* populations will be female biased in response to climate change. That extreme female-bias could affect population growth rate by altering males' fitness with reduction on mate availability given that females individuals have a demographic advantage over males (Haridas et al., 2014; Knight et al., 2005). Further, our work suggest that population viability is sensitive to climate under current and future conditions. This is key because most conservation actions are design from data on current responses to climate, rather than future response to climate (Sletvold et al., 2013). Since the role of male is not negligible in accuralrtly predicting dioecious species response to climate change, management strategies that focus on both sexes would be effective and will enhance our understanding of dioecious species response to global warming.

Conclusion

We have investigated the potential consequence of skewness in sex ratio on population dynamics and range shift in the context of climate change using the Texas bluegrass. We found extreme female -biased in response to climate change. The effect of female biased will induce range shifts to the northern edge of the species current range by limiting mate availability. Beyond, our study case, our results also suggest that tracking only one sex could lead to an underestimation of the effect of climate change on population dynamics. Our work provides also a framework for predicting the impact of global warming on population dynamics using the probability of population to self-sustain.

⁴³⁴ **Acknowledgements**

⁴³⁵ This research was supported by National Science Foundation Division of Environmental
⁴³⁶ Biology awards 2208857 and 2225027. We thank the institutions who hosted us at their field
⁴³⁷ station facilities, including

438 **References**

- 439 Aguilée, R., Raoul, G., Rousset, F., and Ronce, O. (2016). Pollen dispersal slows geographical
440 range shift and accelerates ecological niche shift under climate change. *Proceedings of the
441 National Academy of Sciences*, 113(39):E5741–E5748.
- 442 Alexander, J. M., Diez, J. M., and Levine, J. M. (2015). Novel competitors shape species'
443 responses to climate change. *Nature*, 525(7570):515–518.
- 444 Bertrand, R., Lenoir, J., Piedallu, C., Riofrío-Dillon, G., De Ruffray, P., Vidal, C., Pierrat, J.-C.,
445 and Gégout, J.-C. (2011). Changes in plant community composition lag behind climate
446 warming in lowland forests. *Nature*, 479(7374):517–520.
- 447 Bürkner, P.-C. (2017). brms: An R package for Bayesian multilevel models using Stan. *Journal
448 of Statistical Software*, 80(1):1–28.
- 449 Bruijning, M., Visser, M. D., Muller-Landau, H. C., Wright, S. J., Comita, L. S., Hubbell, S. P.,
450 de Kroon, H., and Jongejans, E. (2017). Surviving in a cosexual world: A cost-benefit
451 analysis of dioecy in tropical trees. *The American Naturalist*, 189(3):297–314.
- 452 Bürli, S., Pannell, J. R., and Tonnabel, J. (2022). Environmental variation in sex ratios and
453 sexual dimorphism in three wind-pollinated dioecious plant species. *Oikos*, 2022(6):e08651.
- 454 Caswell, H. (1989). Analysis of life table response experiments i. decomposition of effects
455 on population growth rate. *Ecological Modelling*, 46(3-4):221–237.
- 456 Caswell, H. (2000). *Matrix population models*, volume 1. Sinauer Sunderland, MA.
- 457 Chen, X., Liang, Y., and Feng, X. (2024). Influence of model complexity, training collinearity,
458 collinearity shift, predictor novelty and their interactions on ecological forecasting. *Global
459 Ecology and Biogeography*, 33(3):371–384.
- 460 Cipollini, M. L. and Whigham, D. F. (1994). Sexual dimorphism and cost of reproduction
461 in the dioecious shrub *lindera benzoin* (lauraceae). *American Journal of Botany*, 81(1):65–75.
- 462 Cleland, E. E., Chuine, I., Menzel, A., Mooney, H. A., and Schwartz, M. D. (2007). Shifting
463 plant phenology in response to global change. *Trends in ecology & evolution*, 22(7):357–365.
- 464 Compagnoni, A., Steigman, K., and Miller, T. E. (2017). Can't live with them, can't live
465 without them? balancing mating and competition in two-sex populations. *Proceedings of
466 the Royal Society B: Biological Sciences*, 284(1865):20171999.

- ⁴⁶⁷ Corlett, R. T. and Westcott, D. A. (2013). Will plant movements keep up with climate change?
⁴⁶⁸ *Trends in ecology & evolution*, 28(8):482–488.
- ⁴⁶⁹ Czachura, K. and Miller, T. E. (2020). Demographic back-casting reveals that subtle
⁴⁷⁰ dimensions of climate change have strong effects on population viability. *Journal of Ecology*,
⁴⁷¹ 108(6):2557–2570.
- ⁴⁷² Dahlgren, J. P., Bengtsson, K., and Ehrlén, J. (2016). The demography of climate-driven and
⁴⁷³ density-regulated population dynamics in a perennial plant. *Ecology*, 97(4):899–907.
- ⁴⁷⁴ Davis, M. B. and Shaw, R. G. (2001). Range shifts and adaptive responses to quaternary
⁴⁷⁵ climate change. *Science*, 292(5517):673–679.
- ⁴⁷⁶ Diez, J. M., Giladi, I., Warren, R., and Pulliam, H. R. (2014). Probabilistic and spatially variable
⁴⁷⁷ niches inferred from demography. *Journal of ecology*, 102(2):544–554.
- ⁴⁷⁸ Duputié, A., Massol, F., Chuine, I., Kirkpatrick, M., and Ronce, O. (2012). How do genetic cor-
⁴⁷⁹ relations affect species range shifts in a changing environment? *Ecology letters*, 15(3):251–259.
- ⁴⁸⁰ Eberhart-Phillips, L. J., Küpper, C., Miller, T. E., Cruz-López, M., Maher, K. H., Dos Remedios,
⁴⁸¹ N., Stoffel, M. A., Hoffman, J. I., Krüger, O., and Székely, T. (2017). Sex-specific early
⁴⁸² survival drives adult sex ratio bias in snowy plovers and impacts mating system and
⁴⁸³ population growth. *Proceedings of the National Academy of Sciences*, 114(27):E5474–E5481.
- ⁴⁸⁴ Ehrlén, J. and Morris, W. F. (2015). Predicting changes in the distribution and abundance
⁴⁸⁵ of species under environmental change. *Ecology letters*, 18(3):303–314.
- ⁴⁸⁶ Elderd, B. D. and Miller, T. E. (2016). Quantifying demographic uncertainty: Bayesian methods
⁴⁸⁷ for integral projection models. *Ecological Monographs*, 86(1):125–144.
- ⁴⁸⁸ Ellis, R. P., Davison, W., Queirós, A. M., Kroeker, K. J., Calosi, P., Dupont, S., Spicer, J. I.,
⁴⁸⁹ Wilson, R. W., Widdicombe, S., and Urbina, M. A. (2017). Does sex really matter? explaining
⁴⁹⁰ intraspecies variation in ocean acidification responses. *Biology letters*, 13(2):20160761.
- ⁴⁹¹ Ellner, S. P., Adler, P. B., Childs, D. Z., Hooker, G., Miller, T. E., and Rees, M. (2022). A critical
⁴⁹² comparison of integral projection and matrix projection models for demographic analysis:
⁴⁹³ Comment. *Ecology*.
- ⁴⁹⁴ Ellner, S. P., Childs, D. Z., Rees, M., et al. (2016). Data-driven modelling of structured
⁴⁹⁵ populations. *A practical guide to the Integral Projection Model*. Cham: Springer.

- 496 Evans, M. E., Merow, C., Record, S., McMahon, S. M., and Enquist, B. J. (2016). Towards
497 process-based range modeling of many species. *Trends in Ecology & Evolution*, 31(11):860–871.
- 498 Field, D. L., Pickup, M., and Barrett, S. C. (2013). Comparative analyses of sex-ratio variation
499 in dioecious flowering plants. *Evolution*, 67(3):661–672.
- 500 Freeman, D. C., Klikoff, L. G., and Harper, K. T. (1976). Differential resource utilization by
501 the sexes of dioecious plants. *Science*, 193(4253):597–599.
- 502 Gamelon, M., Grøtan, V., Nilsson, A. L., Engen, S., Hurrell, J. W., Jerstad, K., Phillips, A. S.,
503 Røstad, O. W., Slagsvold, T., Walseng, B., et al. (2017). Interactions between demography
504 and environmental effects are important determinants of population dynamics. *Science
505 Advances*, 3(2):e1602298.
- 506 Gerber, L. R. and White, E. R. (2014). Two-sex matrix models in assessing population viability:
507 when do male dynamics matter? *Journal of Applied Ecology*, 51(1):270–278.
- 508 Gissi, E., Bowyer, R. T., and Bleich, V. C. (2024). Sex-based differences affect conservation.
509 *Science*, 384(6702):1309–1310.
- 510 Gissi, E., Schiebinger, L., Hadly, E. A., Crowder, L. B., Santoleri, R., and Micheli, F. (2023).
511 Exploring climate-induced sex-based differences in aquatic and terrestrial ecosystems to
512 mitigate biodiversity loss. *nature communications*, 14(1):4787.
- 513 Haridas, C., Eager, E. A., Rebarber, R., and Tenhumberg, B. (2014). Frequency-dependent
514 population dynamics: Effect of sex ratio and mating system on the elasticity of population
515 growth rate. *Theoretical Population Biology*, 97:49–56.
- 516 Hatfield, J. and Prueger, J. (2015). Temperature extremes: effect on plant growth and
517 development. *weather clim extrem* 10: 4–10.
- 518 Hernández, C. M., Ellner, S. P., Adler, P. B., Hooker, G., and Snyder, R. E. (2023). An exact
519 version of life table response experiment analysis, and the r package exactltre. *Methods
520 in Ecology and Evolution*, 14(3):939–951.
- 521 Hitchcock, A. S. (1971). *Manual of the grasses of the United States*, volume 2. Courier Corporation.
- 522 Hultine, K. R., Grady, K. C., Wood, T. E., Shuster, S. M., Stella, J. C., and Whitham, T. G. (2016).
523 Climate change perils for dioecious plant species. *Nature Plants*, 2(8):1–8.

- 524 Iler, A. M., Compagnoni, A., Inouye, D. W., Williams, J. L., CaraDonna, P. J., Anderson, A., and
525 Miller, T. E. (2019). Reproductive losses due to climate change-induced earlier flowering are
526 not the primary threat to plant population viability in a perennial herb. *Journal of Ecology*,
527 107(4):1931–1943.
- 528 Jones, M. H., Macdonald, S. E., and Henry, G. H. (1999). Sex-and habitat-specific responses
529 of a high arctic willow, *salix arctica*, to experimental climate change. *Oikos*, pages 129–138.
- 530 Karger, D. N., Conrad, O., Böhner, J., Kawohl, T., Kreft, H., Soria-Auza, R. W., Zimmermann,
531 N. E., Linder, H. P., and Kessler, M. (2017). Climatologies at high resolution for the earth's
532 land surface areas. *Scientific data*, 4(1):1–20.
- 533 Kindiger, B. (2004). Interspecific hybrids of *poa arachnifera* × *poa secunda*. *Journal of New
534 Seeds*, 6(1):1–26.
- 535 Knight, T. M., Steets, J. A., Vamosi, J. C., Mazer, S. J., Burd, M., Campbell, D. R., Dudash,
536 M. R., Johnston, M. O., Mitchell, R. J., and Ashman, T.-L. (2005). Pollen limitation of plant
537 reproduction: pattern and process. *Annu. Rev. Ecol. Evol. Syst.*, 36:467–497.
- 538 Konapala, G., Mishra, A. K., Wada, Y., and Mann, M. E. (2020). Climate change will affect
539 global water availability through compounding changes in seasonal precipitation and
540 evaporation. *Nature communications*, 11(1):3044.
- 541 Kremer, A., Ronce, O., Robledo-Arnuncio, J. J., Guillaume, F., Bohrer, G., Nathan, R., Bridle,
542 J. R., Gomulkiewicz, R., Klein, E. K., Ritland, K., et al. (2012). Long-distance gene flow and
543 adaptation of forest trees to rapid climate change. *Ecology letters*, 15(4):378–392.
- 544 Lee-Yaw, J. A., Kharouba, H. M., Bontrager, M., Mahony, C., Csergő, A. M., Noreen, A. M.,
545 Li, Q., Schuster, R., and Angert, A. L. (2016). A synthesis of transplant experiments and
546 ecological niche models suggests that range limits are often niche limits. *Ecology letters*,
547 19(6):710–722.
- 548 Liaw, A., Wiener, M., et al. (2002). Classification and regression by randomforest. *R news*,
549 2(3):18–22.
- 550 Louthan, A. M., Keighron, M., Kiekebusch, E., Cayton, H., Terando, A., and Morris, W. F.
551 (2022). Climate change weakens the impact of disturbance interval on the growth rate of
552 natural populations of venus flytrap. *Ecological Monographs*, 92(4):e1528.

- 553 Lynch, H. J., Rhainds, M., Calabrese, J. M., Cantrell, S., Cosner, C., and Fagan, W. F. (2014).
554 How climate extremes—not means—define a species' geographic range boundary via a
555 demographic tipping point. *Ecological Monographs*, 84(1):131–149.
- 556 McLean, N., Lawson, C. R., Leech, D. I., and van de Pol, M. (2016). Predicting when climate-
557 driven phenotypic change affects population dynamics. *Ecology Letters*, 19(6):595–608.
- 558 Merow, C., Bois, S. T., Allen, J. M., Xie, Y., and Silander Jr, J. A. (2017). Climate change both
559 facilitates and inhibits invasive plant ranges in new england. *Proceedings of the National
560 Academy of Sciences*, 114(16):E3276–E3284.
- 561 Miller, T. and Compagnoni, A. (2022a). Data from: Two-sex demography, sexual niche
562 differentiation, and the geographic range limits of texas bluegrass (*Poa arachnifera*). *American
563 Naturalist, Dryad Digital Repository*,. <https://doi.org/10.5061/dryad.kkwh70s5x>.
- 564 Miller, T. E. and Compagnoni, A. (2022b). Two-sex demography, sexual niche differentiation,
565 and the geographic range limits of texas bluegrass (*poa arachnifera*). *The American
566 Naturalist*, 200(1):17–31.
- 567 Miller, T. E., Shaw, A. K., Inouye, B. D., and Neubert, M. G. (2011). Sex-biased dispersal and
568 the speed of two-sex invasions. *The American Naturalist*, 177(5):549–561.
- 569 Morrison, C. A., Robinson, R. A., Clark, J. A., and Gill, J. A. (2016). Causes and consequences
570 of spatial variation in sex ratios in a declining bird species. *Journal of Animal Ecology*,
571 85(5):1298–1306.
- 572 Pease, C. M., Lande, R., and Bull, J. (1989). A model of population growth, dispersal and
573 evolution in a changing environment. *Ecology*, 70(6):1657–1664.
- 574 Petry, W. K., Soule, J. D., Iler, A. M., Chicas-Mosier, A., Inouye, D. W., Miller, T. E., and
575 Mooney, K. A. (2016). Sex-specific responses to climate change in plants alter population
576 sex ratio and performance. *Science*, 353(6294):69–71.
- 577 Piironen, J. and Vehtari, A. (2017). Comparison of bayesian predictive methods for model
578 selection. *Statistics and Computing*, 27:711–735.
- 579 Pottier, P., Burke, S., Drobniak, S. M., Lagisz, M., and Nakagawa, S. (2021). Sexual (in) equality?
580 a meta-analysis of sex differences in thermal acclimation capacity across ectotherms.
581 *Functional Ecology*, 35(12):2663–2678.

- 582 Pulliam, H. R. (2000). On the relationship between niche and distribution. *Ecology letters*,
583 3(4):349–361.
- 584 R Core Team (2023). *R: A Language and Environment for Statistical Computing*. R Foundation
585 for Statistical Computing, Vienna, Austria.
- 586 Reed, P. B., Peterson, M. L., Pfeifer-Meister, L. E., Morris, W. F., Doak, D. F., Roy, B. A., Johnson,
587 B. R., Bailes, G. T., Nelson, A. A., and Bridgman, S. D. (2021). Climate manipulations
588 differentially affect plant population dynamics within versus beyond northern range limits.
589 *Journal of Ecology*, 109(2):664–675.
- 590 Renganayaki, K., Jessup, R., Burson, B., Hussey, M., and Read, J. (2005). Identification of
591 male-specific AFLP markers in dioecious Texas bluegrass. *Crop science*, 45(6):2529–2539.
- 592 Sanderson, B. M., Knutti, R., and Caldwell, P. (2015). A representative democracy to reduce
593 interdependency in a multimodel ensemble. *Journal of Climate*, 28(13):5171–5194.
- 594 Schultz, E. L., Hülsmann, L., Pillet, M. D., Hartig, F., Breshears, D. D., Record, S., Shaw, J. D.,
595 DeRose, R. J., Zuidema, P. A., and Evans, M. E. (2022). Climate-driven, but dynamic and
596 complex? a reconciliation of competing hypotheses for species' distributions. *Ecology letters*,
597 25(1):38–51.
- 598 Schwalm, C. R., Glendon, S., and Duffy, P. B. (2020). Rcp8.5 tracks cumulative CO₂ emissions.
599 *Proceedings of the National Academy of Sciences*, 117(33):19656–19657.
- 600 Schwinning, S., Lortie, C. J., Esque, T. C., and DeFalco, L. A. (2022). What common-garden
601 experiments tell us about climate responses in plants.
- 602 Sexton, J. P., McIntyre, P. J., Angert, A. L., and Rice, K. J. (2009). Evolution and ecology of
603 species range limits. *Annu. Rev. Ecol. Evol. Syst.*, 40:415–436.
- 604 Shelton, A. O. (2010). The ecological and evolutionary drivers of female-biased sex ratios:
605 two-sex models of perennial seagrasses. *The American Naturalist*, 175(3):302–315.
- 606 Sherry, R. A., Zhou, X., Gu, S., Arnone III, J. A., Schimel, D. S., Verburg, P. S., Wallace,
607 L. L., and Luo, Y. (2007). Divergence of reproductive phenology under climate warming.
608 *Proceedings of the National Academy of Sciences*, 104(1):198–202.
- 609 Sletvold, N. and Ågren, J. (2015). Climate-dependent costs of reproduction: Survival and
610 fecundity costs decline with length of the growing season and summer temperature.
611 *Ecology Letters*, 18(4):357–364.

- 612 Sletvold, N., Dahlgren, J. P., Øien, D.-I., Moen, A., and Ehrlén, J. (2013). Climate warming
613 alters effects of management on population viability of threatened species: results from
614 a 30-year experimental study on a rare orchid. *Global Change Biology*, 19(9):2729–2738.
- 615 Smith, M. D., Wilkins, K. D., Holdrege, M. C., Wilfahrt, P., Collins, S. L., Knapp, A. K., Sala,
616 O. E., Dukes, J. S., Phillips, R. P., Yahdjian, L., et al. (2024). Extreme drought impacts have
617 been underestimated in grasslands and shrublands globally. *Proceedings of the National
618 Academy of Sciences*, 121(4):e2309881120.
- 619 Stan Development Team (2023). RStan: the R interface to Stan. R package version 2.21.8.
- 620 Thomson, A. M., Calvin, K. V., Smith, S. J., Kyle, G. P., Volke, A., Patel, P., Delgado-Arias,
621 S., Bond-Lamberty, B., Wise, M. A., Clarke, L. E., et al. (2011). Rcp4. 5: a pathway for
622 stabilization of radiative forcing by 2100. *Climatic change*, 109:77–94.
- 623 Tognetti, R. (2012). Adaptation to climate change of dioecious plants: does gender balance
624 matter? *Tree Physiology*, 32(11):1321–1324.
- 625 Williams, J. L., Jacquemyn, H., Ochocki, B. M., Brys, R., and Miller, T. E. (2015). Life
626 history evolution under climate change and its influence on the population dynamics of
627 a long-lived plant. *Journal of Ecology*, 103(4):798–808.

Supporting Information

628 S.1 Supporting Figures

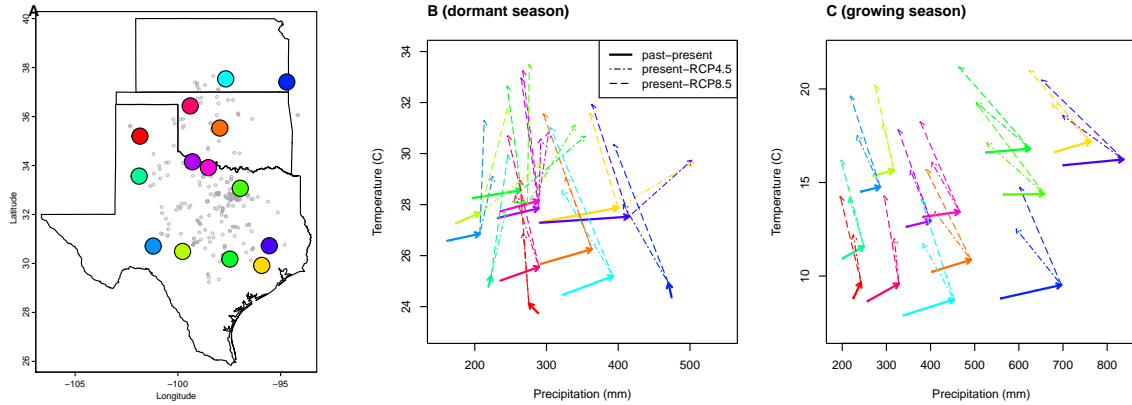


Figure S-1: (A), Common garden locations in Texas, Oklahoma, and Kansas (points) and (B,C) corresponding changes in growing and dormant season climate. Arrows in B,C connect past (1901-1930) and present (1990-2019) climate normals, and present and future (2071-2100) climate normals under RCP4.5 and RCP8.5 forecasts. Future forecasts are from MIROC5 but other climate models show similar patterns.

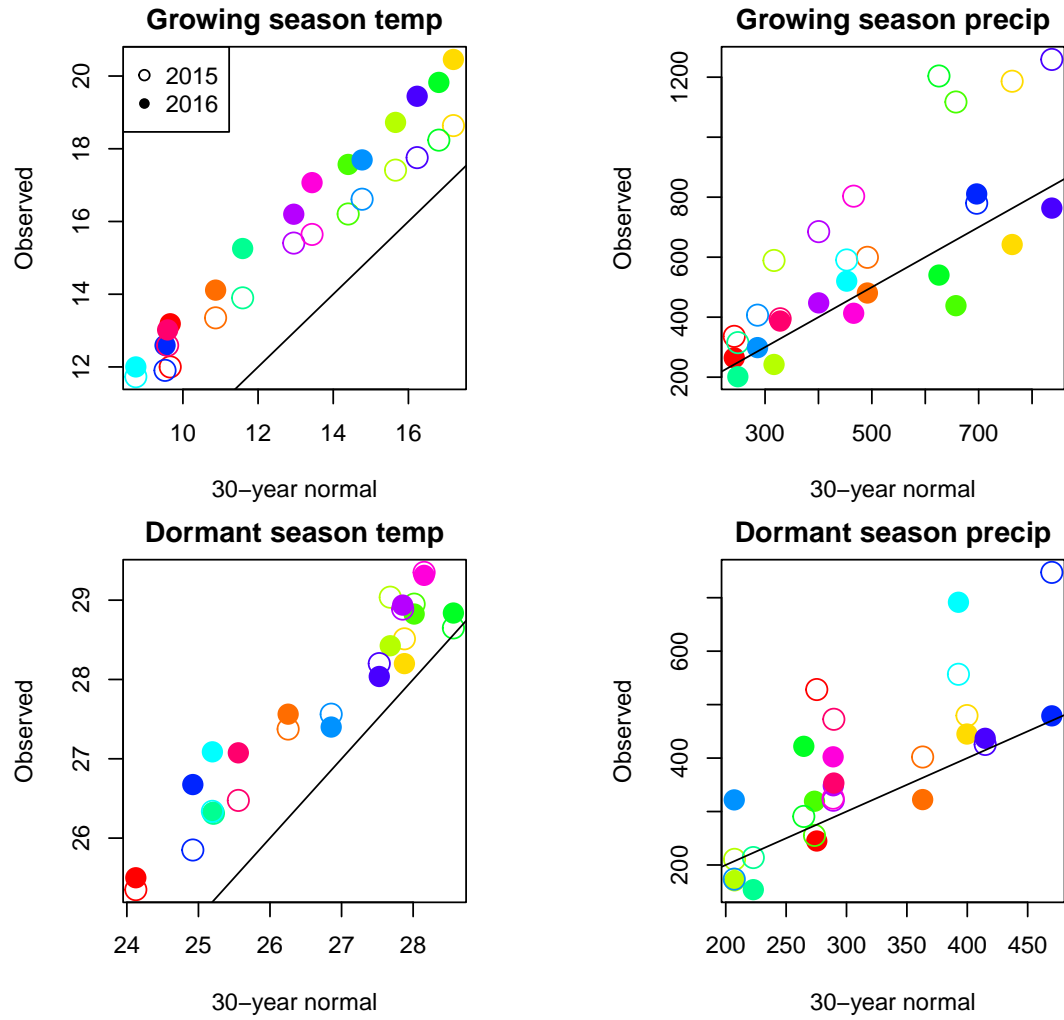


Figure S-2: Comparison of 30-year (1990-2019) climate normals and observed weather conditions at common garden sites during the 2014–15 and 2015–16 census periods. Temperature is in $^{\circ}\text{C}$ and precipitation is in mm . Colors represent sites and lines show the $y=x$ relationship.

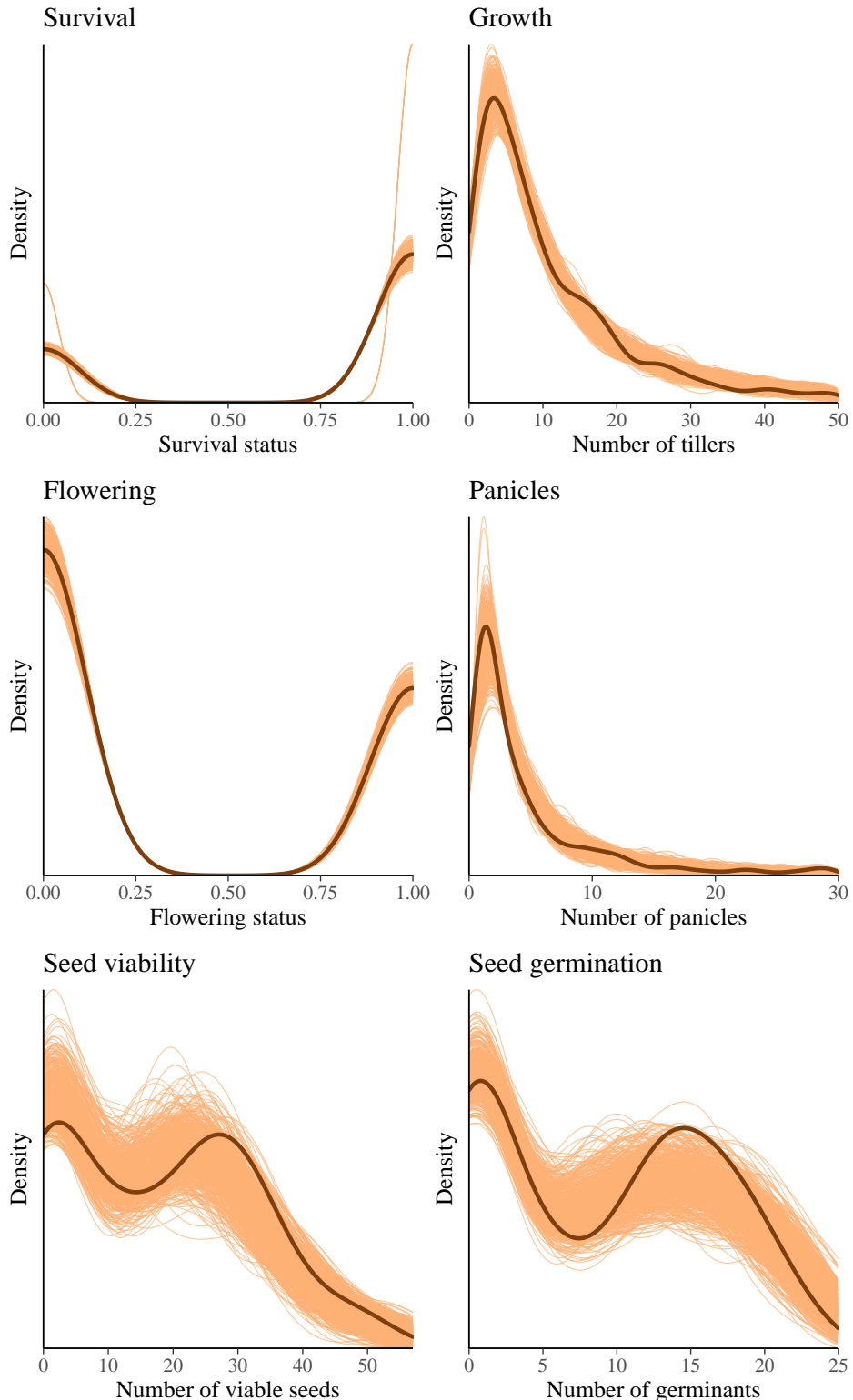


Figure S-3: Posterior predictive checks. Consistency between real data and simulated values suggests that the fitted vital rate models accurately describes the data. Graph shows density curves for the observed data (light orange) along with the simulated values (dark orange).

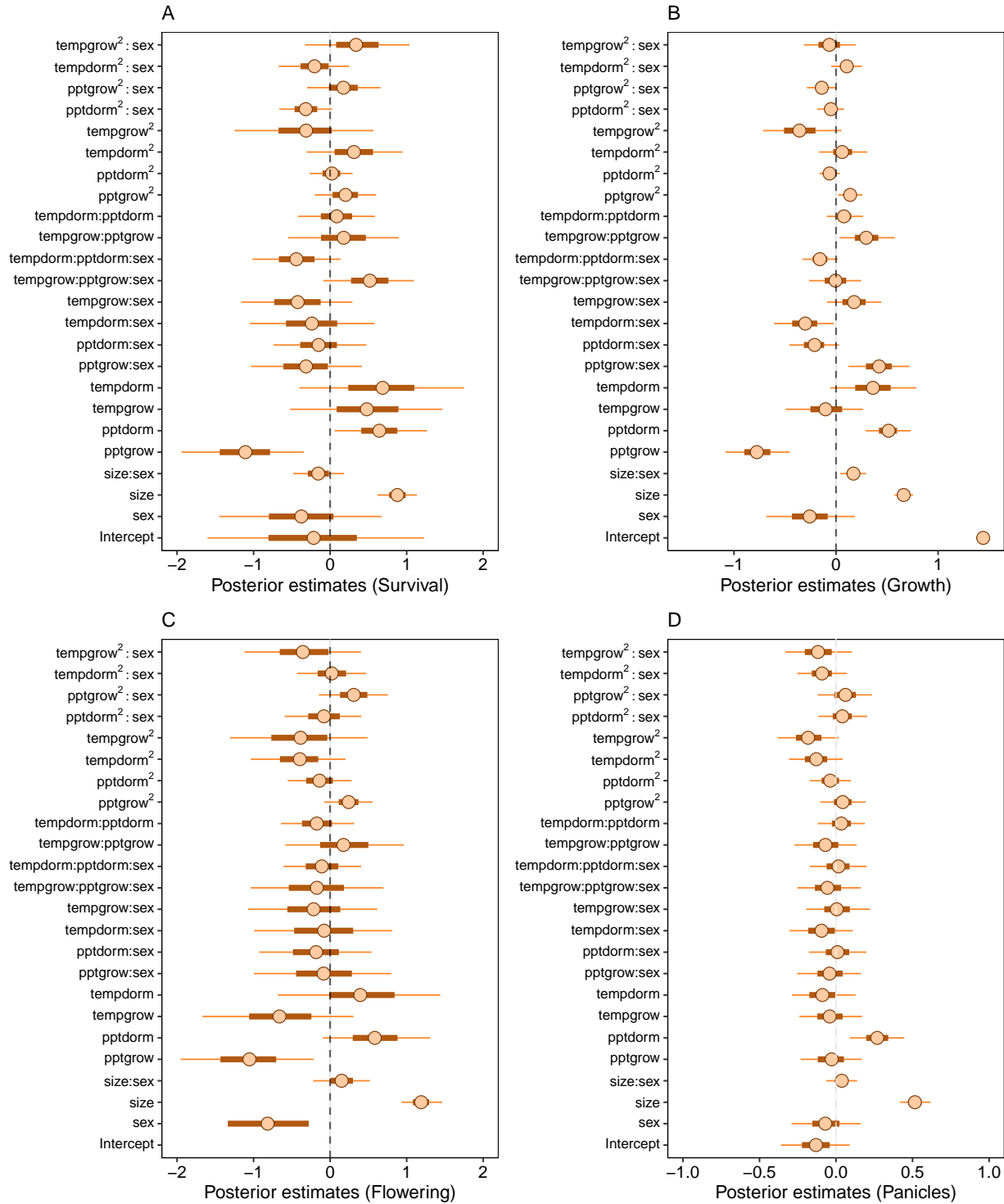


Figure S-4: Mean parameter values and 95% credible intervals of the posterior probability distributions. pptgrow is the precipitation of growing season, Tempgrow is the temperature of growing season, pptdorm is the temperature of dormant season, Tempdorm is the temperature of dormant season.

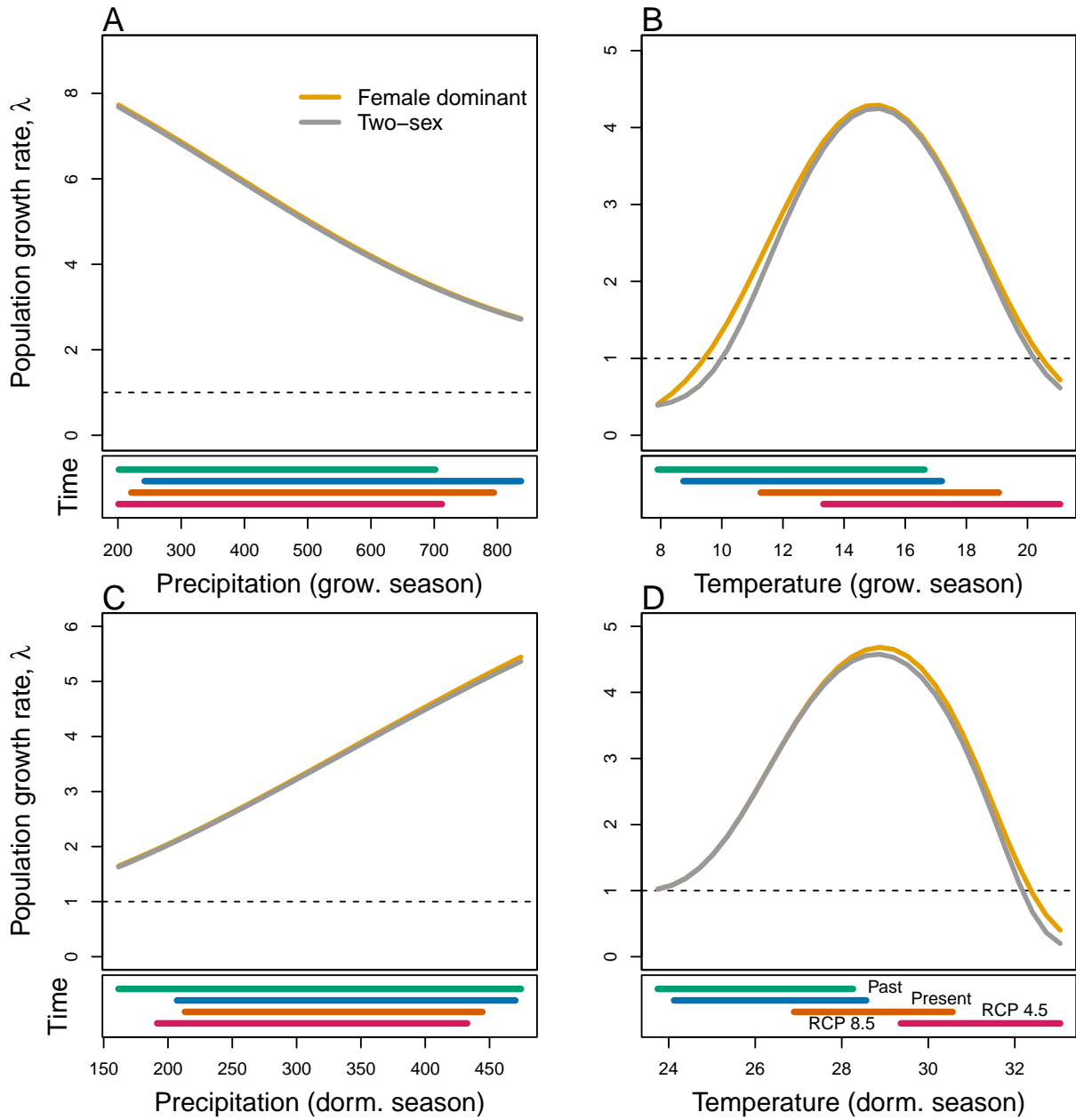


Figure S-5: Predicted population growth rate (λ) in different ranges of climate. (A) Precipitation of the growing season, (B) Temperature of the growing season, (C) Precipitation of the dormant season, (D) Temperature of the dormant season. The grey curve shows prediction by the two-sex matrix projection model that incorporates sex-specific demographic responses to climate with sex ratio dependent seed fertilization. The orange curve represents the prediction by the female dominant matrix projection model. The dashed horizontal line indicates the limit of population viability ($\lambda = 1$). Lower panels below each data panel show ranges of climate values for different time period (past climate, present and future climates). For future climate, we show a Representation Concentration Pathways (RCP) 4.5 and 8.5. Values of (λ) are derived from the mean climate variables across 4 GCMs (MIROC5, ACCESS1-3, CESM1-BGC, CMCC-CM).

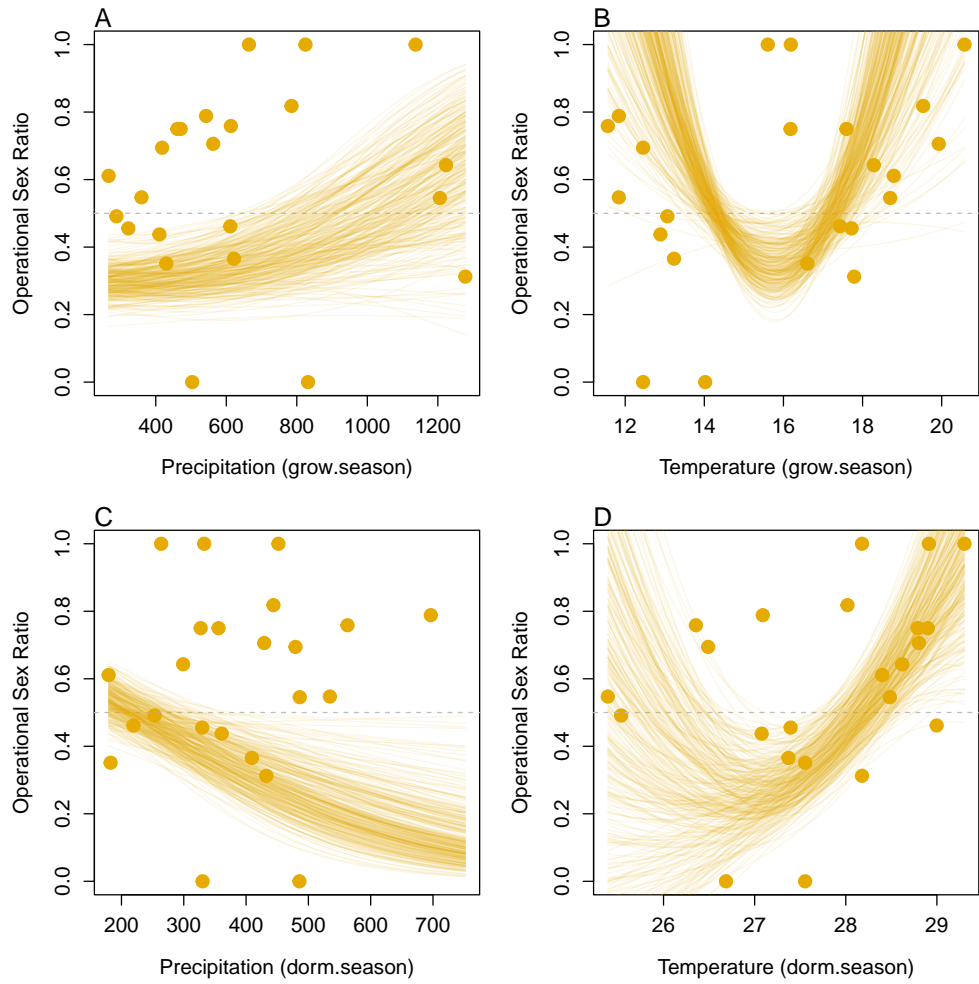


Figure S-6: Significant Operational Sex Ratio response across climate gradient. (A, B) Proportion of panicles that were females across precipitation and temperature of the growing season; (C, D) Proportion of panicles that were females across precipitation and temperature of the dormant season.

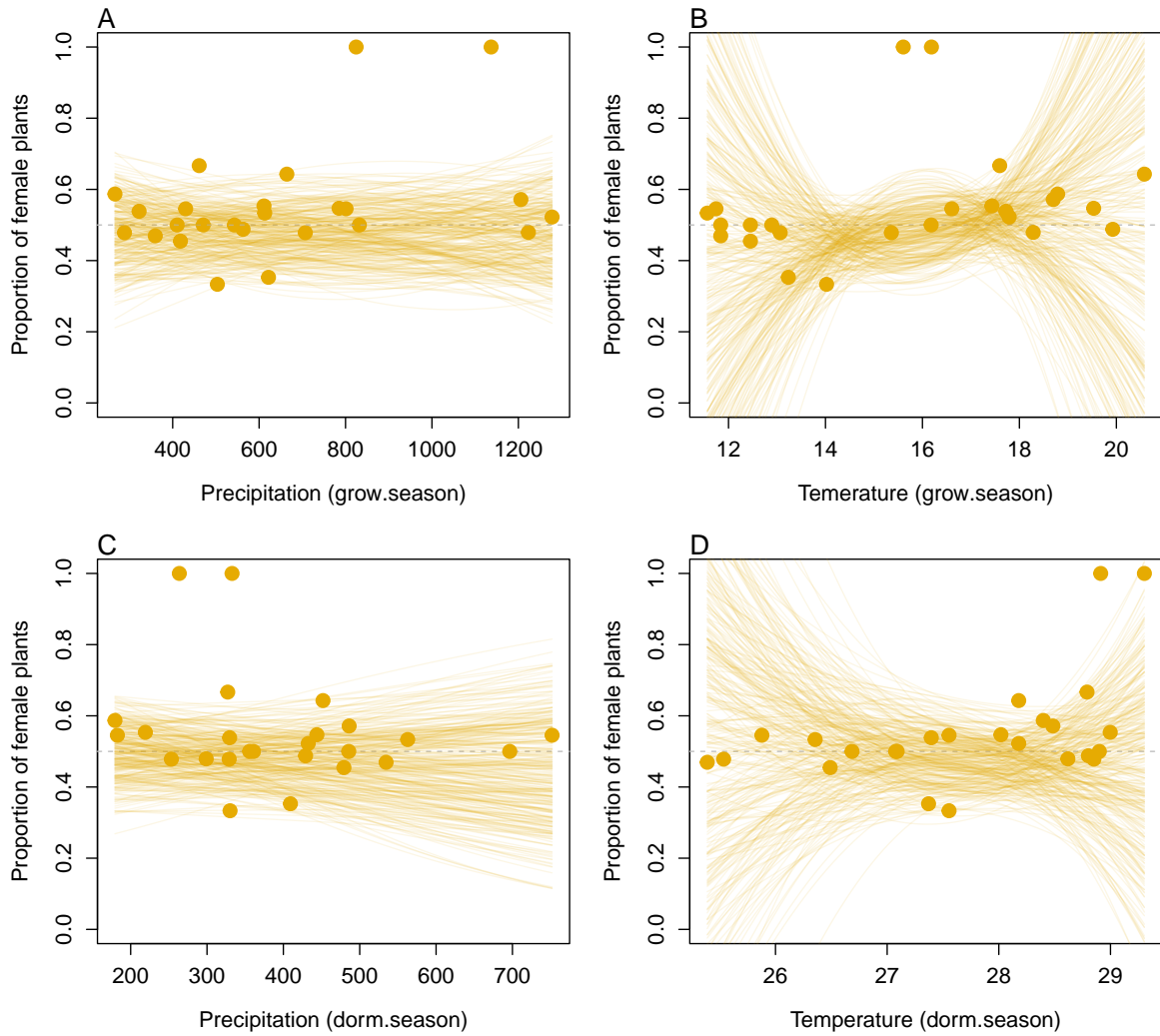


Figure S-7: Variation in sex-ratio across climate gradient. (A, B) Proportion of plants that were females across precipitation and temperature of the growing season; (C, D) Proportion of plants that were females across precipitation and temperature of the dormant season.

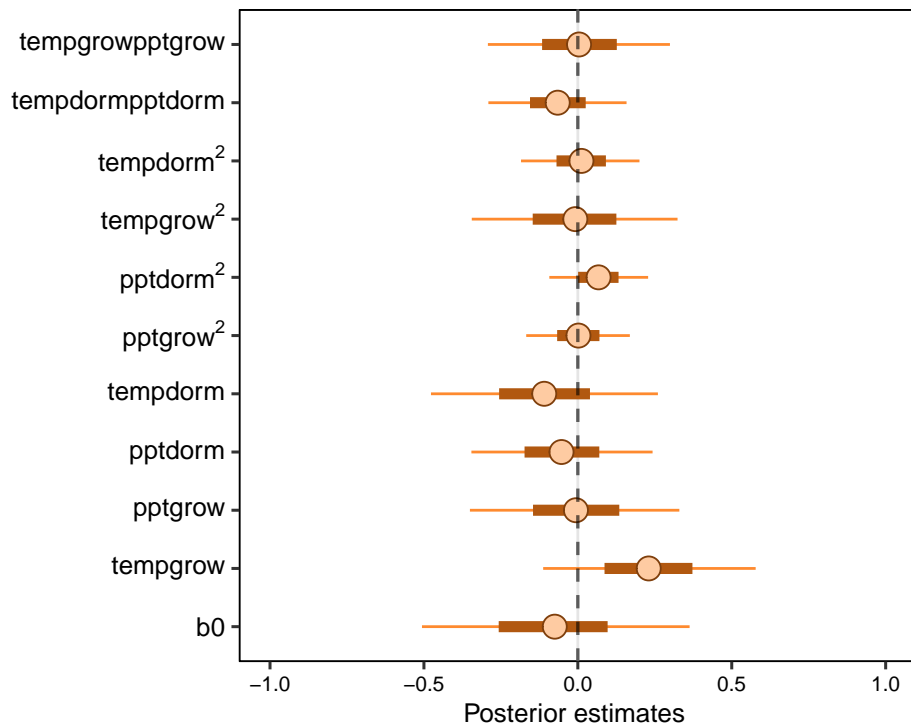


Figure S-8: Mean parameter values and 95% credible intervals of the posterior probability distributions. pptgrow is the precipitation of growing season, Tempgrow is the temperature of growing season, pptdorm is the temperature of dormant season, Tempdorm is the temperature of dormant season.

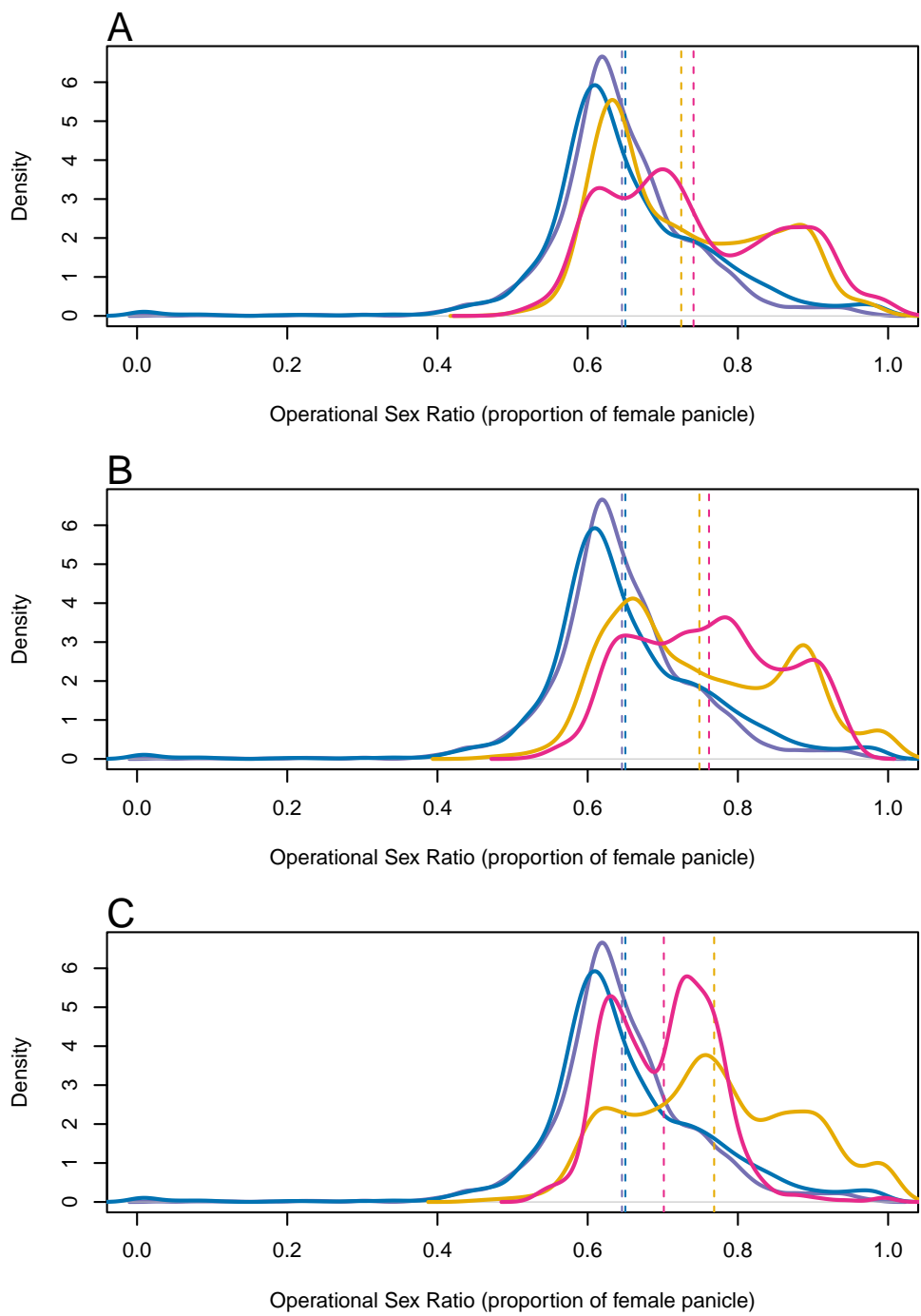


Figure S-9: Change in Operational Sex Ratio (proportion of female) over time (past, present, future). Future projections were based on A) MIROC 5, B) CES, C) ACC. The means for each model are shown as vertical dashed lines.

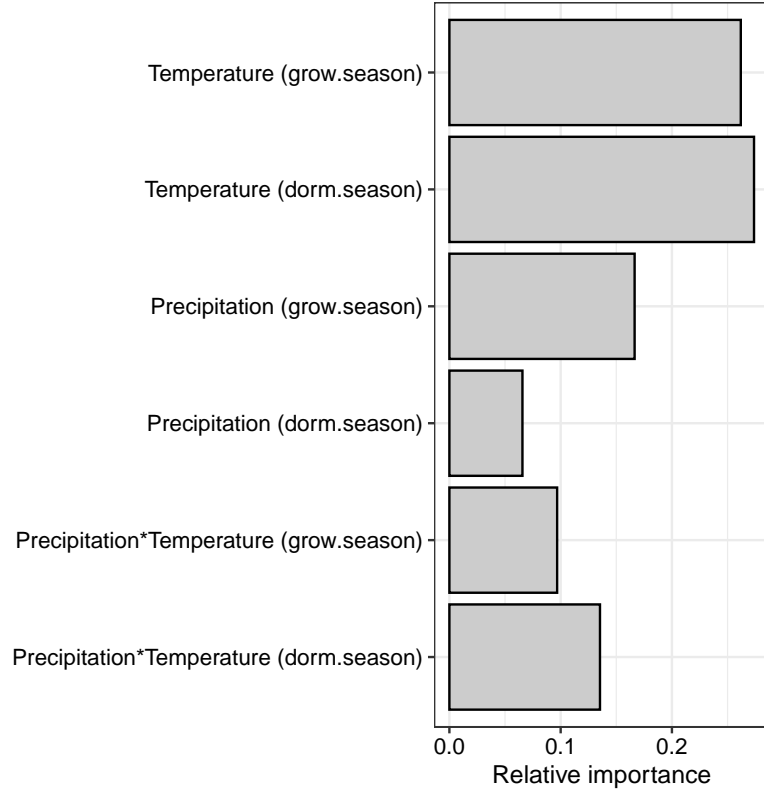


Figure S-10: Life Table Response Experiment: The bar represent the relative importance of each predictors.

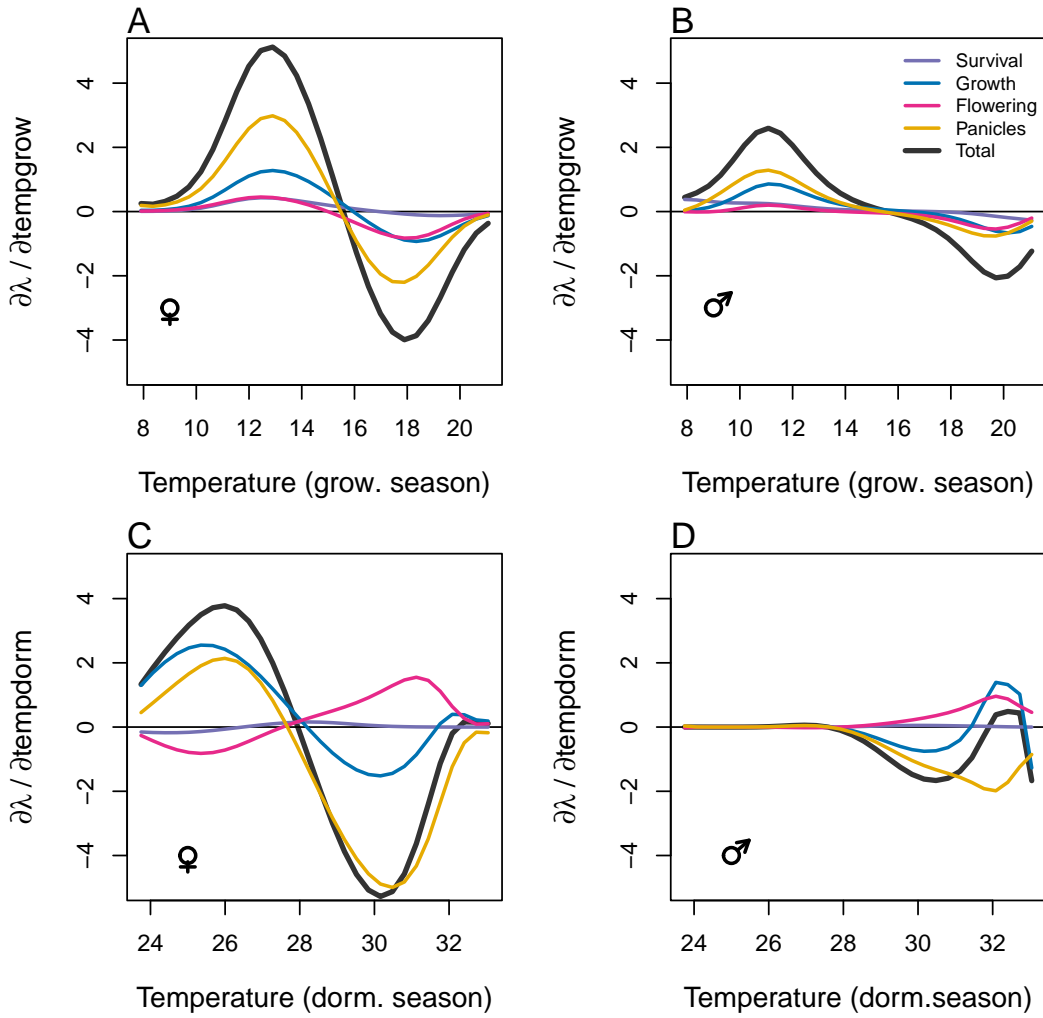


Figure S-11: Life table response experiment decomposition of the sensitivity of λ to seasonal climate into additive vital rate contributions of males and females based on posterior mean parameter estimates. (A) Temperature of growing season (contribution of female), (B) Temperature of growing season (contribution of male), (C) Temperature of dormant season (contribution of female) and (D) Temperature of dormant season (contribution of male).

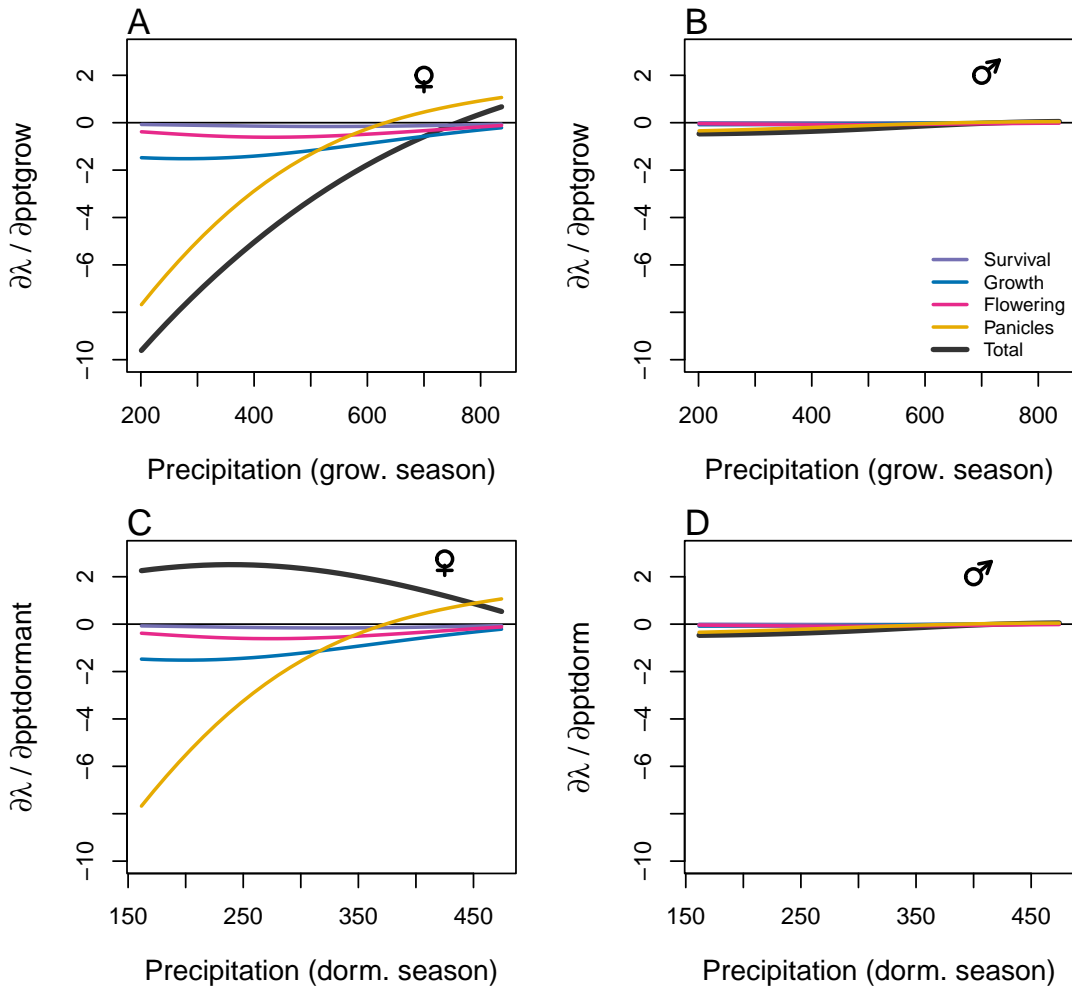


Figure S-12: Life table response experiment decomposition of the sensitivity of λ to seasonal climate into additive vital rate contributions of males and females based on posterior mean parameter estimates. (A) Precipitation of growing season (contribution of female), (B) Precipitation of growing season (contribution of male), (C) Precipitation of dormant season (contribution of female) and (D) Precipitation of dormant season (contribution of male).

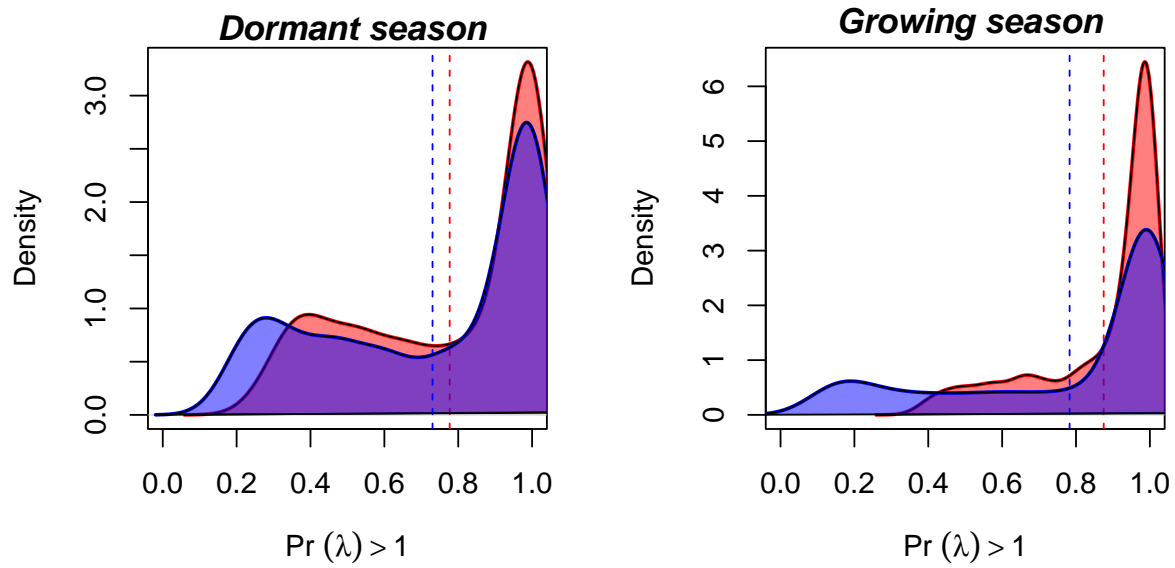


Figure S-13: Assessment of the statistical difference between the two-sex models and the female dominant model for the dormant and growing season. Plots show the density of $\Pr(\lambda) > 1$ values for female dominant (pink) and two-sex models (violet) for each season. The means for each model are shown as vertical dashed lines.

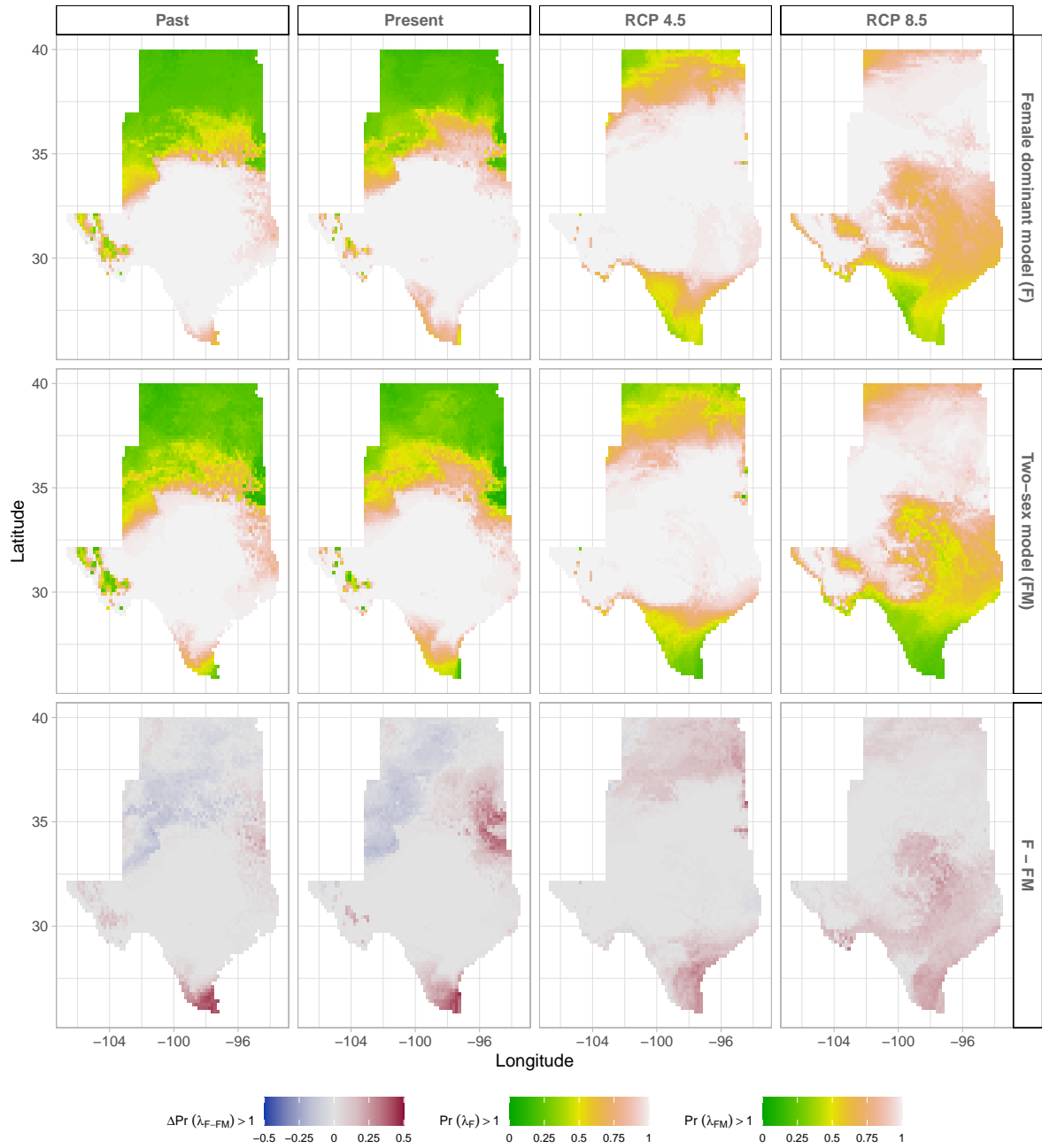


Figure S-14: Climate change favors range shift toward the North edge of the current range. (A) Past, (B) Current, (C and D) Future predicted range shift based on the predicted probabilities of self- sustaining populations, $\Pr(\lambda > 1)$, using the two-sex model that incorporates sex- specific demographic responses to climate with sex ratio dependent seed fertilization. (E) Past, (F) Current, (G and H) Future predicted range shift based on the predicted probabilities of self- sustaining populations, $\Pr(\lambda > 1)$, using the female dominant model. Future projections were based on the CESM1-BGC model. The black dots on panel B and F indicate all known presence points collected from GBIF from 1990 to 2019, which corresponds to the current condition in our prediction. The occurrences of GBIFs are distributed in with higher population fitness habitat $\Pr(\lambda > 1)$, confirming that our study approach can reasonably predict range shifts.

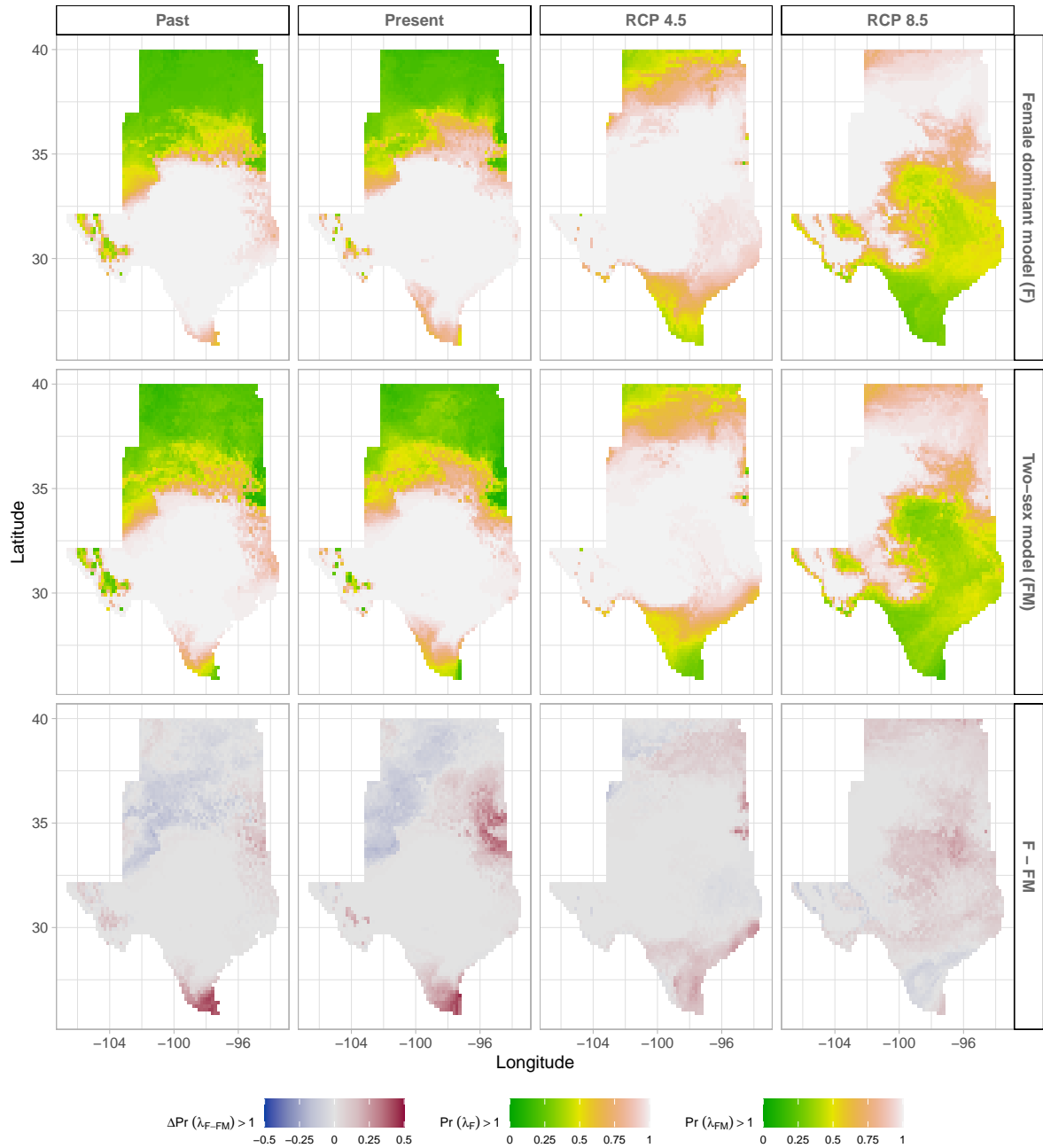


Figure S-15: Climate change favors range shift toward the North edge of the current range. (A) Past, (B) Current, (C and D) Future predicted range shift based on the predicted probabilities of self- sustaining populations, $\text{Pr}(\lambda > 1)$, using the two-sex model that incorporates sex- specific demographic responses to climate with sex ratio dependent seed fertilization. (E) Past, (F) Current, (G and H) Future predicted range shift based on the predicted probabilities of self- sustaining populations, $\text{Pr}(\lambda > 1)$, using the female dominant model. Future projections were based on the ACCESS model. The black dots on panel B and F indicate all known presence points collected from GBIF from 1990 to 2019, which corresponds to the current condition in our prediction. The occurrences of GBIFs are distributed in with higher population fitness habitat $\text{Pr}(\lambda > 1)$, confirming that our study approach can reasonably predict range shifts.

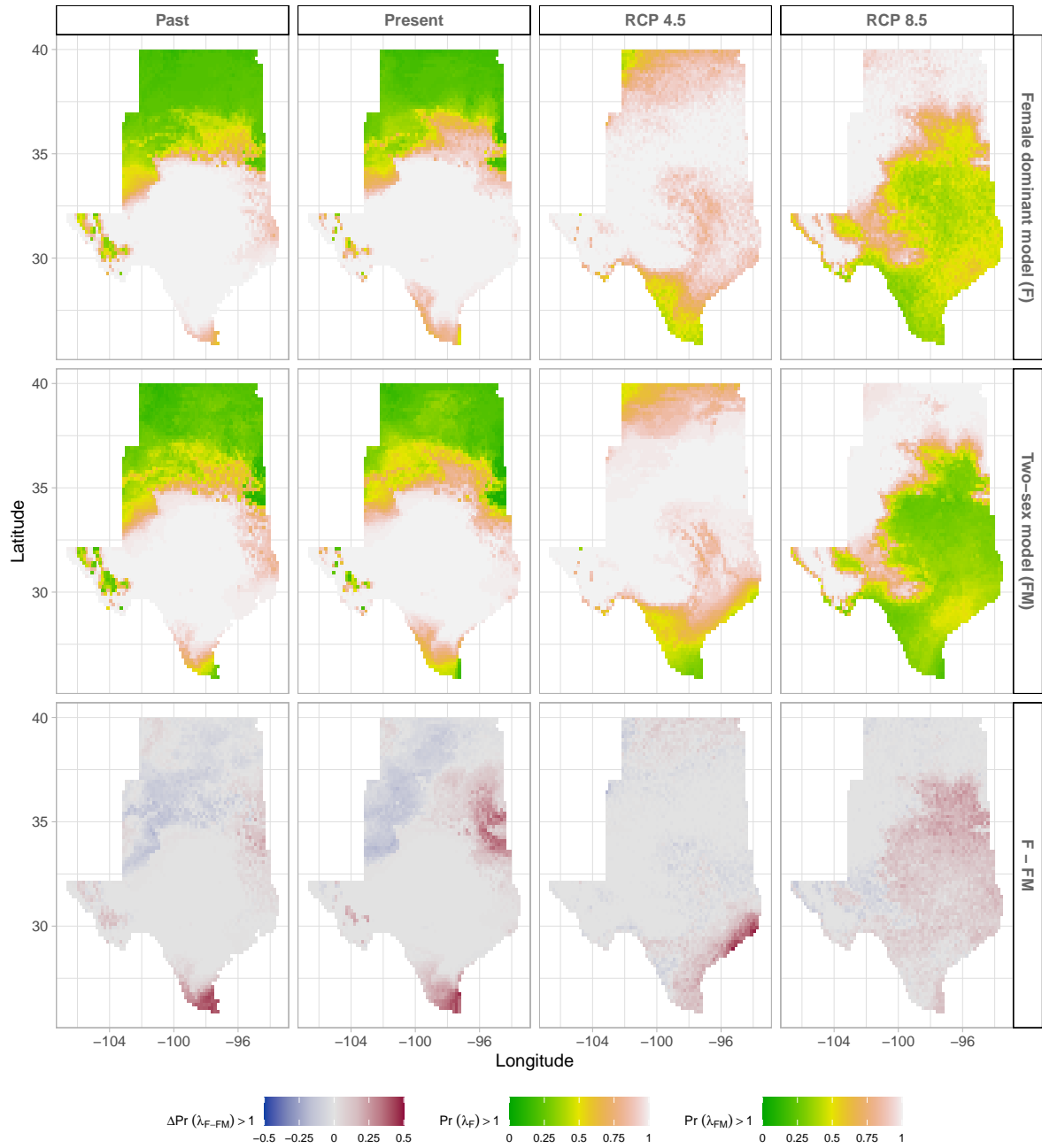


Figure S-16: Climate change favors range shift toward the North edge of the current range. (A) Past, (B) Current, (C and D) Future predicted range shift based on the predicted probabilities of self- sustaining populations, $\text{Pr}(\lambda > 1)$, using the two-sex model that incorporates sex- specific demographic responses to climate with sex ratio dependent seed fertilization. (E) Past, (F) Current, (G and H) Future predicted range shift based on the predicted probabilities of self- sustaining populations, $\text{Pr}(\lambda > 1)$, using the female dominant model. Future projections were based on the MIROC5 model. The black dots on panel B and F indicate all known presence points collected from GBIF from 1990 to 2019, which corresponds to the current condition in our prediction. The occurrences of GBIFs are distributed in with higher population fitness habitat $\text{Pr}(\lambda > 1)$, confirming that our study approach can reasonably predict range shifts.

629 **S.2 Supporting Methods**

630 **Sex ratio experiment**

To estimate the probability of seed viability, the germination rate and the effect of sex-ratio variation on female reproductive success, we conducted a sex-ratio experiment at one site near the center of the range to estimate the effect of sex-ratio variation on female reproductive success. The details of the experiment are provided in Compagnoni et al. (2017) and Miller and Compagnoni (2022b). Here we provide a summary of the experiment. We established 124 experimental populations in plots measuring 0.4 × 0.4m and separated by at least 15m from each other. We varied population density (1-48 plants/plot) and sex ratio (0%-100% female) across the experimental populations, and we replicated 34 combinations of density and sex ratio. We collected panicles from a subset of females in each plot and recorded the number of seeds in each panicle. We assessed reproductive success (seeds fertilized) using greenhouse-based germination and trazolium-based seed viability assays. Seed viability was modeled with a binomial distribution where the probability of viability (v) was given by:

$$v = v_0 * (1 - OSR^\alpha) \quad (\text{S.1})$$

631 where OSR is the proportion of panicles that were female in the experimental populations.
632 α is the parameter that control for how viability declines with increasing female bias. Further,
633 germination rate was modeled using a binomial distribution to model the germination
634 data from greenhouse trials. Given that germination was conditional on seed viability, the
635 probability of success was given by the product $v * g$, where v is a function of OSR (Eq. S.1)
636 and g is assumed to be constant.